AGT

Algebraic & Geometric Topology

Volume 25 (2025)

# Cocycles of the space of long embeddings and BCR graphs with more than one loop

LEO YOSHIOKA

msp

msp

*Algebraic & Geometric Topology* **25**:6 (2025) 3385–3427
DOI: 10.2140/agt.2025.25.3385
Published: 1 October 2025

# Cocycles of the space of long embeddings and BCR graphs with more than one loop

LEO YOSHIOKA

The purpose of this paper is to construct nontrivial cocycles of the space $\mathrm{Emb}(\mathbb{R}^j, \mathbb{R}^n)$ of long embeddings. We construct the cocycles through configuration space integrals, associated with Bott–Cattaneo–Rossi graphs with more than one loop. As an application, we give a nontrivial cycle of long embeddings in the path component of the trivial long embedding, for odd $n$, $j$ with $n - j \geq 2$ and $j \geq 3$. This cycle is constructed from a chord diagram on directed lines. The nontriviality is shown by cocycle-cycle pairing, described by pairing between graphs and chord diagrams.

57K16, 57K45, 57M15, 57R40

Introduction 3385
1. Background 3387
2. Definitions 3388
3. Main result 3397
4. Construction of the cocycles 3399
5. Review of Sakai and Watanabe's construction of the wheel-like cycles 3404
6. Construction of the cycles 3407
7. Some lemmas for computing cocycle-cycle pairing 3417
8. Proof of the main result 3423
References 3425

## Introduction

A long embedding is an embedding of $\mathbb{R}^j$ into $\mathbb{R}^n$, which is standard outside a disk in $\mathbb{R}^j$. A long $n$-knot is a long embedding $\mathbb{R}^n \to \mathbb{R}^{n+2}$. In this paper, we produce some geometric nontrivial cocycles of the space $\mathrm{Emb}(\mathbb{R}^j, \mathbb{R}^n)$ of long embeddings through integrals associated with graphs. This kind of approach, which we call configuration space integrals, has its quantum field theoretical origin in E Witten's work [39] and its mathematical formulation has been developed by M Kontsevich [18], D Bar-Natan [5], R Bott [6], C Taubes [7], G Kuperberg, D Thurston [19], A S Cattaneo and C A Rossi [11] and some others from the

© 2025 MSP (Mathematical Sciences Publishers). Distributed under the Creative Commons Attribution License 4.0 (CC BY). Open Access made possible by subscribing institutions via Subscribe to Open.

1990s to 2000s. Recently, this approach attracted much attention thanks to T Watanabe [36], who in 2018 disproved the 4-dimensional Smale conjecture based on a series of his works [33; 34; 35].

Bott [6] and Cattaneo and Rossi [11] defined 1-loop graphs (graphs with $b_1 = 1$) with two types of edges and vertices. We call these graphs BCR graphs. Using specific linear combinations of BCR graphs called graph cocycles, they defined configuration space integral invariants for long $n$-knots. K Sakai and Watanabe [27; 29] generalized their construction and systematically gave nontrivial higher cocycles of $\mathrm{Emb}(\mathbb{R}^j, \mathbb{R}^n)$ for $n - j \geq 3$ from BCR graph cocycles.

The graphs used in this paper are similar to theirs, but our graphs have more than one loop ($b_1 \geq 2$). Using such higher-loop graphs plays an essential role in getting cocycles of higher degree when the codimension $n - j$ is exactly two. The framework of applying higher-loop BCR graphs was already considered by Sakai [27]. However, no nontrivial cocycle corresponding to higher-loop graphs has been given so far.

In this paper, we show the following. (See Section 3.)

**Theorem 0.1** *Let $n, j$ be odd and satisfy $n - j \geq 2$ and $j \geq 3$. Then the linear combination $H$ of 2-loop BCR graphs gives an explicit nontrivial $3n - 2j - 7$ (co)cycle of $\overline{\mathrm{Emb}}(\mathbb{R}^j, \mathbb{R}^n)$, the space of long embeddings modulo immersions.*

This theorem is shown by cocycle-cycle pairing. We systematically construct cycles of the space of long embeddings, which we call generalized ribbon cycles, from chord diagrams on directed lines. This diagrammatic construction makes it possible to compute cocycle-cycle pairing through pairing between graphs and diagrams. This diagrammatic computation is analogous to the diagrammatic description of cohomology-homology pairing of configuration spaces that D P Sinha introduced in [31].

As a corollary, we give a nontrivial $S^2$-family of trivial long 3-knots. Budney and Gabai [9] and Watanabe [37] already showed that the $(n-1)^{\mathrm{st}}$ homotopy group of the path component of the trivial long $n$-knots, $\pi_{n-1}(\mathrm{Emb}(\mathbb{R}^n, \mathbb{R}^{n+2})_\iota)$ ($n \geq 2$), has an infinite-rank subgroup, by different approaches from ours. However, their families of long $n$-knots are constructed through $\mathrm{Diff}_\partial(D^{n+1} \times S^1)$ or $\mathrm{Emb}_\partial(D^1, D^{n+1} \times S^1)$. It would be interesting to compare our construction of families with theirs. Note that our approach has the possibility to produce an infinite-rank subgroup of $\pi_{n-1}(\mathrm{Emb}(\mathbb{R}^n, \mathbb{R}^{n+2})_\iota)$ using more general 2-loop graphs.

Moreover, our graph cocycles with more than one loop further support the interesting similarity between the BCR graph complex and the graph complex introduced by G Arone and V Turchin [2; 3]. Their complex arises from a homotopy theoretical approach to embedding spaces: embedding calculus developed by Goodwillie, Klein and Weiss [14; 15; 38]. The significant point of their complex is that its graph homology has the full information about the dimension of the rational homology of $\mathrm{Emb}(\mathbb{R}^j, \mathbb{R}^n)$ for $n \geq 2j + 2$.[1] They mentioned in [3] that some of their graphs are very similar to BCR graphs with no

[1] In [13], Fresse, Turchin and Willwacher generalized the results of [3] to $n - j \geq 3$. Note that their approach consists of the Goodwillie–Weiss embedding calculus tower and its mapping space model. The latter is applicable to any codimension, though the former works for $n - j \geq 3$.

more than one loop. The point there was that Arone and Turchin's graph complex allows graphs with any number of loops. The 2-loop graph cocycle we give in this paper has the 2-loop graph

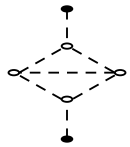

similar to a graph which appears as a nontrivial element in [3]. Since BCR graph cohomology can give information for any codimension more than one, we would be able to say that the stability of high codimensions that is described by this graph also survives in the range $n - j = 2$.

Although we can apply our framework to the case when $n$ and $j$ are even, we have got no nontrivial cocycles of the space of long embeddings. The main cause is that we have not got a nontrivial graph cocycle for $n$, $j$ even. But one will be able to guess nontrivial cocycles from the computation of the 2-loop part of Arone and Turchin's graph homology [12]. Note that the graph homology is infinite dimensional.

The paper is organized as follows. First, in Section 1, we review the framework of configuration space integrals associated with BCR graphs. After that, some definitions and notation are given in Section 2. The main result is stated in Section 3. Then in Section 4, we construct the well-defined cocycles of $\mathrm{Emb}(\mathbb{R}^n, \mathbb{R}^{n+2})$. After reviewing Sakai and Watanabe's construction of cycles in Section 5, we construct cycles from chord diagrams on directed lines in Section 6. In Section 7, we show preliminary lemmas used in the proof of the main result. Finally, in Section 8, we give the proof of the main result by pairing the cocycles and the cycles of Sections 4 and 6, described by graph-diagram pairing.

**Acknowledgements**

The author is deeply grateful to the author's supervisor, Mikio Furuta, for his continuous support and encouragement for years. The author would like to thank Tadayuki Watanabe for explaining much of his work; discussion with Watanabe was highly motivating during the preparation of this paper. The author thanks Keiichi Sakai for the great opportunity to talk and discuss at the Shinshu Topology Seminar. Sakai also taught the author a lot about embedding spaces. The author also thanks Masahito Yamazaki and Tatsuro Shimizu for helpful suggestions and stimulating conversations. The author thanks Victor Turchin for sharing the papers [12; 13] and for advice for better exposition.

This research was supported by the Forefront Physics and Mathematics Program to Drive Transformation (FoPM), a World-leading Innovative Graduate Study (WINGS) program, at the University of Tokyo.

# 1 Background

## 1.1 The BCR graph complex and the de Rham complex of $\mathrm{Emb}(\mathbb{R}^j, \mathbb{R}^n)$

Sakai [27] defined the BCR graph complex $(\mathcal{D}_g^{k,l}, \delta)$ and constructed a linear map from this space to the de Rham complex of $\mathrm{Emb}(\mathbb{R}^j, \mathbb{R}^n)$ through configuration space integrals. This correspondence

gives a higher dimensional analog (in the sense $j \geq 2$) of the correspondence developed by Cattaneo, Cotta-Ramusino and Longoni [10]. Refer to Sections 2.2 and 2.3 for the definition of the BCR graph complex (and the definitions of $k$, $g$ and $l$).

**Theorem 1.1** [27, Theorem 1.2] *Let $k \geq 1$ and $g \geq 0$. Configuration space integrals give a linear map*

$$I : \mathcal{D}_g^{k,l} \to \Omega_{dR}^{k(n-j-2)+(g-1)(j-1)+l}(\mathrm{Emb}(\mathbb{R}^j, \mathbb{R}^n)).$$

*Moreover, if either*

- *$n-j$ is even, $n-j \geq 2$, $j \geq 2$ and $g = 0$, or*
- *$n$ and $j$ are odd, $n > j \geq 3$ and $g = 1$,*

*then the map $I$ gives a cochain map.*

Based on the above theorem, it is expected that we can obtain nontrivial cohomology classes of $\mathrm{Emb}(\mathbb{R}^j, \mathbb{R}^n)$ if the graph cohomology is nontrivial and the map on the cohomology level induced from $I$ satisfies injectivity.

From this perspective, Sakai and Watanabe conducted further research on $g = 1$ (and $l = 0$) in [29], where configuration space integral invariants are put together into the universal one. Their work is based on the theory of finite type invariants for ribbon $n$-knots developed by Habiro, Kanenobu and Shima [17; 16].

**Theorem 1.2** [29, Theorem 1.1] *Let $(n, j, k)$ satisfy some conditions. Let $\mathcal{A}_1^k$ be the quotient of the space of 1-loop graphs by some relations (such as the STU relations of Jacobi diagrams). Then there exists a linear and injective map*

$$\alpha : \mathcal{A}_1^k \to H_{(n-j-2)k}(\mathrm{Emb}(\mathbb{R}^j, \mathbb{R}^n), \mathbb{R}).$$

*In fact, the universal configuration space integral invariant $z_k$ gives a closed $(n-j-2)k$ form, and detects the nontriviality of the above cycles. We review the construction of the cycles in Section 5.*

**Remark 1.3** In Theorem 1.1, we can observe that when $n - j = 2$ we have to use graphs with $g \geq 2$ or $l \geq 1$ to obtain cocycles of higher degree.

**Remark 1.4** The case $l \geq 1$ is out of the scope of this paper. For the case $j = 1$, some progress has been made by Longoni [23], Sakai [26; 28], and Pelatt and Sinha [25]. In these works, new types of cycles are constructed generalizing the case $l = 0$.

## 2 Definitions

### 2.1 The space of long embeddings

First, We define the space of long embeddings and some related spaces.

**Definition 2.1** A long embedding is an embedding $\mathbb{R}^j \to \mathbb{R}^n$ which coincides with the standard linear embedding $\iota\colon \mathbb{R}^j \subset \mathbb{R}^n$ outside a disk in $\mathbb{R}^j$. A long embedding $\mathbb{R}^n \to \mathbb{R}^{n+2}$ is called a long $n$-knot. We equip the space $\mathrm{Emb}(\mathbb{R}^j, \mathbb{R}^n)$ of long embeddings with the induced topology from the weak $C^\infty$ topology. We define the space of long immersions $\mathrm{Imm}(\mathbb{R}^j, \mathbb{R}^n)$ similarly.

**Remark 2.2** Budney showed in [8] that $\mathrm{Emb}(S^j, S^n) \simeq \mathrm{SO}_{n+1} \times_{\mathrm{SO}_{n-j}} \mathrm{Emb}(\mathbb{R}^j, \mathbb{R}^n)$. That is, the difference between the two spaces $\mathrm{Emb}(S^j, S^n)$ and $\mathrm{Emb}(\mathbb{R}^j, \mathbb{R}^n)$ is given by the Stiefel manifold $\mathrm{SO}_{n+1}/\mathrm{SO}_{n-j}$, whose homotopy groups are well-studied.

**Remark 2.3** We often consider $\mathrm{Emb}_\partial(D^j, D^n)$, the space of embeddings $D^j \to D^n$ which are standard near the boundary, instead of $\mathrm{Emb}(\mathbb{R}^j, \mathbb{R}^n)$. The homotopy types of these two spaces are equivalent.

For technical reasons, sometimes we think of the space of embeddings modulo immersions.

**Definition 2.4** We write $\overline{\mathrm{Emb}}(\mathbb{R}^j, \mathbb{R}^n)$ for the homotopy fiber of the inclusion

$$\mathrm{Emb}(\mathbb{R}^j, \mathbb{R}^n) \hookrightarrow \mathrm{Imm}(\mathbb{R}^j, \mathbb{R}^n)$$

at the standard linear embedding $\iota\colon \mathbb{R}^j \subset \mathbb{R}^n$. That is, an element of $\overline{\mathrm{Emb}}(\mathbb{R}^j, \mathbb{R}^n)$ is a one-parameter family $\{\overline{K}_t\}_{t\in[0,1]}$ of long immersions which satisfies $\overline{K}_0 = \iota$, $\overline{K}_1 \in \mathrm{Emb}(\mathbb{R}^j, \mathbb{R}^n)$. Let

$$r\colon \overline{\mathrm{Emb}}(\mathbb{R}^j, \mathbb{R}^n) \to \mathrm{Emb}(\mathbb{R}^j, \mathbb{R}^n)$$

be the natural projection.

**Notation 2.5** Write $\iota\colon \mathbb{R}^j \to \mathbb{R}^n$ for the standard linear embedding. The path component of $\mathrm{Emb}(\mathbb{R}^j, \mathbb{R}^n)$ which $\iota$ belongs to is denoted by $\mathrm{Emb}(\mathbb{R}^j, \mathbb{R}^n)_\iota$. We often call this component the unknot component. Write $\overline{\mathrm{Emb}}(\mathbb{R}^j, \mathbb{R}^n)_\iota$ for the component of the trivial family of the standard linear immersion.

## 2.2 BCR graphs

We move on to the definition of BCR graphs and their complex. See Section 3 for examples of BCR graphs. Although we basically follow the definitions of [6; 11; 27; 29; 32], we restate them since there are some differences in conventions among these papers.

**Definition 2.6** A BCR graph is a graph which satisfies the following conditions.

(1) There are two types of vertices, white and black.

(2) There are two types of edges, dashed and solid.

(3) Each white vertex has only dashed edges, and its valency is at least three. Each black vertex has at least one dashed edge and has an arbitrary number of solid edges.

(4) White vertices have no small loop:

Black vertices have no small loop consisting of a solid edge only:

(See Remark 2.8 below.)

**Example 2.7** Here are typical examples of vertices of BCR graphs:

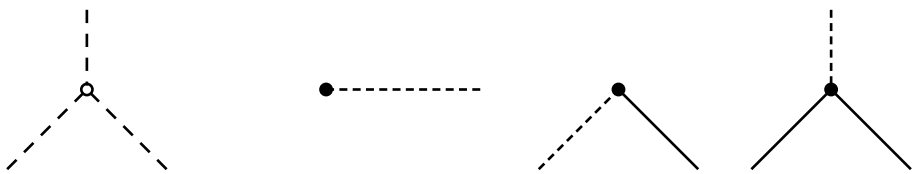

**Remark 2.8** Black vertices are allowed to have small loops:

and double loops:

We write the set of small loops of $\Gamma$ as $L_s(\Gamma)$ and the set of double loops as $L_d(\Gamma)$. Set $L(\Gamma) = L_s(\Gamma) \sqcup L_d(\Gamma)$. In our case ($n$ and $j$ are odd), double loops vanish by the third relation in Definition 2.19.

**Notation 2.9** Let $\Gamma$ be a BCR graph. We denote the set of solid edges of $\Gamma$ by $E_\eta(\Gamma)$, and the set of dashed edges by $E_\theta(\Gamma)$. Edges of small loops and double loops are included in these sets. The set of edges $E(\Gamma)$ is decomposed as

$$E(\Gamma) = E_\eta(\Gamma) \sqcup E_\theta(\Gamma).$$

We denote the set of black vertices of $\Gamma$ by $B(\Gamma)$, and the set of white vertices by $W(\Gamma)$. The set of vertices $V(\Gamma)$ is decomposed as

$$V(\Gamma) = B(\Gamma) \sqcup W(\Gamma).$$

**Definition 2.10** (defect of a graph) Let $v$ be a vertex of a BCR graph $\Gamma$. We define the defect $l(v)$ of $v$ as

$$l(v) = \begin{cases} \#E_\theta(v) - 3 & \text{if } v \in W(\Gamma), \\ \#E_\theta(v) - 1 & \text{if } v \in B(\Gamma). \end{cases}$$

Here $E_\theta(v)$ is the number of dashed edges $v$ has. The defect $l(\Gamma)$ of $\Gamma$ is defined as

$$l(\Gamma) = \sum_{v \in V(\Gamma)} l(v),$$

and is equal to

$$2\#E_\theta(\Gamma) - 3\#W(\Gamma) - \#B(\Gamma).$$

**Remark 2.11** The defect of a graph measures how the graph is different, in terms of edge contractions, from graphs in which each black vertex has exactly one dashed edge and each white vertex has exactly three dashed edges.

**Definition 2.12** (order of a graph) The order $k(\Gamma)$ of a BCR graph $\Gamma$ is given by

$$k(\Gamma) = \#E_\theta(\Gamma) - \#W(\Gamma).$$

**Remark 2.13** When the defect is 0, we have $k = \frac{1}{2}\#V(\Gamma)$.

**Definition 2.14** ($g$-loop graphs) A BCR graph is a $g$-loop graph if the first Betti number of any component is $g$. Here, we consider small and double loops as points, and we do not count them as loops.

**Definition 2.15** (labels of a graph) We give a label of $\Gamma$ by an ordering of $V(\Gamma)$, an ordering of $E(\Gamma)$, an orientation of each edge $e \in E(\Gamma)$ and an ordering of $L_s(\Gamma)$. Here, an ordering of a set $X$ with $m$ elements is a bijective map from $\{1, 2, \dots, m\}$ to $X$. We choose an ordering so that black vertices and solid edges come first.

**Definition 2.16** (orientations of a graph) An orientation $s$ of a graph $\Gamma$ is a choice

$$s \in \det\left(\mathbb{R}V(\Gamma) \oplus \bigoplus_{e \in E(\Gamma)} \mathbb{R}H(e)\right).$$

Here $H(e)$ is the set of two half-edges of $e$. A labeled graph determines an orientation of the underlying graph.

**Remark 2.17** In this paper, we only handle the case $n$ and $j$ are odd. The above definitions of labels and orientations are only for this case. We can define orientation of graphs so that the definition depends only on the parities of $n$ and $j$.

**Remark 2.18** An ordering of $L_s(\Gamma)$ is used to define the configuration space integral associated with $\Gamma$. However, since we define configuration space integrals for graphs of defect 0, we do not use this data in the rest of this paper.

## 2.3 The BCR graph complex

**Definition 2.19** We define relations of the vector space spanned by labeled BCR graphs of order $k$ and defect $l$. We denote the quotient space by $\mathcal{D}^{k,l}$.

(1) Two labels with the same orientation are identified, and ones with opposite orientations are given opposite signs.

(2) $\Gamma = 0$ for any graph $\Gamma$ with a double edge:

(3) $\Gamma = 0$ for any graph $\Gamma$ with a double loop. (On the other hand, a graph with small loops may survive.)

(4) When $l = 0$, we set $\Gamma = 0$ for any "nonadmissible" graph $\Gamma$. A graph $\Gamma$ is nonadmissible
   (i) if it has a black vertex whose eta-valency is at least three, such as

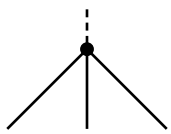

   (ii) if it has a multiple edge

**Notation 2.20** We write the subspace of $\mathcal{D}^{k,l}$ generated by graphs with $g$ loops as $\mathcal{D}_g^{k,l}$. (Here, we count neither small nor double loops as loops.)

**Remark 2.21** The fourth condition is just to make the computation of the top cohomology easier, and it follows the conventions of [29]. So far, the author has yet to find precise reasons to exclude the possibility that we can construct a graph cocycle (of defect 0) essentially using these nonadmissible graphs. But one possible reason is that we can change nonadmissible graphs to admissible graphs by the Arnold relation (see Section 2.4) with respect to solid edges.

**Remark 2.22** One possible variant of $\mathcal{D}$ is the graph complex $\overline{\mathcal{D}}$ that is the same as $\mathcal{D}$ for $l \geq 0$ but has defect $(-1)$ part $\overline{\mathcal{D}}^{-1}$. Here a graph with defect $(-1)$ is a graph that has vertices of defect 0 and exactly one black vertex with three solid edges and no dashed edge. Contractions of the three solid edges adjacent to the black vertex yield the Arnold relation.

Next, we define the coboundary map $\delta\colon \mathcal{D}_g^{k,l} \to \mathcal{D}_g^{k,l+1}$ of the graph complex.

**Definition 2.23** (contraction of a BCR graph [27]) We define the contraction $\Gamma/e$ of a BCR graph $\Gamma$ at an edge $e$ as follows.

(a) When $e = (p, q) \in E_\eta(\Gamma)$ (except multiple edges).

Collapse $e$ to the black vertex at the ends of $e$ with a smaller label, and then reassign labels to vertices of the collapsed graph in a natural way (that is, assign $\min\{p, q\}$ to this collapsed vertex, and subtract 1 from all vertex-labels greater than $\max\{p, q\}$):

(b) When $e=(p,q)\in E_\theta(\Gamma)$ and at least one of $p$ and $q$ is white.

If exactly one is white, collapse $e$ to the black vertex. If both are white, collapse $e$ to the white vertex with a smaller label. The way to reassign labels is similar to (a):

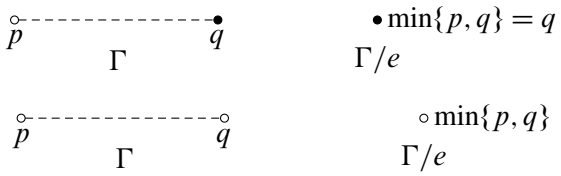


(c) When $e=(p,q)\in E_\theta(\Gamma)$ and both $p$ and $q$ are black vertices.

We construct a small loop.[2] If the number of small loops of $\Gamma$ is $a$, the label of this loop is $(a+1)$:

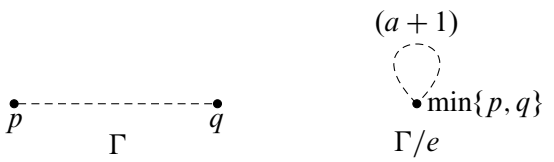


(d) When $e=(p,q)$ is the solid edge of a multiple edge.

We construct a double loop, which vanishes by the third relation in Definition 2.19. We do not perform contractions of dashed edges of multiple edges.

**Definition 2.24** (coboundary map [27]) We define the coboundary map $\delta\colon \mathcal{D}_g^{k,l}\to\mathcal{D}_g^{k,l+1}$ of $\mathcal{D}_g^{k,l}$ as

$$\delta(\Gamma)=\sum_{e\in E(\Gamma)\setminus\{\text{loops}\}}\sigma(e)\Gamma/e.$$

Here, the sign $\sigma(e)$ of an edge $e$ is defined as

$$\sigma(e=(p,q))=\begin{cases}(-1)^q & \text{if } p<q,\\ (-1)^{p+1} & \text{if } p>q.\end{cases}$$

**Proposition 2.25** *$(\mathcal{D}_g^{k,*},\delta)$ is a cochain complex.*

**Proof** This follows from the fact that reversing the order of two contractions changes the sign. □

## 2.4 Comparing with the Arone–Turchin graph complex

Arone and Turchin [2; 3] defined two graph complexes $\mathcal{C}^{j,n}$ and $HH^{j,n}$ ($j$ and $n$ come from $\mathrm{Emb}(\mathbb{R}^j,\mathbb{R}^n)$). These complexes both arise from a homotopy theoretical approach: the description of the space of long embeddings as a space of derived maps between modules over an operad.

[2] Though [27] introduces sign of small loops, it seems unnecessary.

The complex $\mathscr{E}^{j,n}$ consists of so-called hairy graphs with two types of vertices and with one type of edges. Graphs of $HH^{j,n}$ have two types of edges as graphs of $\mathscr{D}$. The differences between $HH^{j,n}$ and our complex $\mathscr{D} = \mathscr{D}^{j,n}$ are:

(1) Their graphs have only black vertices.

(2) Their graphs do not have cycles that consist of one type of edges. In particular, there are no small loops, double loops or double edges.

(3) Their coboundary map is the sum of contractions of only solid edges.

(4) Their complex has another relation called the Arnold relation [1] as follows (the edges in the figure must be the same type, either dashed or solid):

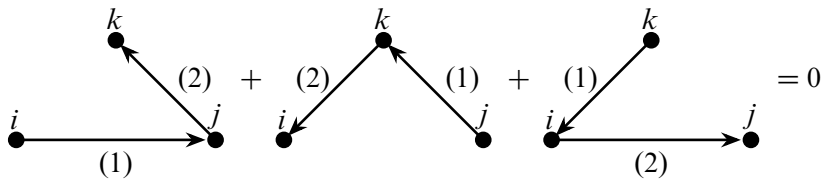


Note that our convention for solid and dashed edges are opposite from [2; 3]: we follow the convention that solid edges correspond to $\mathbb{R}^j$ of the domain.

## 2.5 Configuration space integrals

From now on, for simplicity, we assume that graphs used to define configuration space integrals are connected and satisfy $l = 0$.

**Notation 2.26** We write $C_s(\mathbb{R}^n)$ for the configuration space of $s$ points in $\mathbb{R}^n$:

$$C_s(\mathbb{R}^n) = (\mathbb{R}^n)^s \setminus \text{all diagonals}.$$

**Definition 2.27** (configuration space) Let $K\colon \mathbb{R}^j \to \mathbb{R}^n$ be a long embedding. Then we define the configuration space $C_{s,t}(K, \mathbb{R}^n)$ as

$$C_{s,t}(K, \mathbb{R}^n) = \{(x_1, x_2, \dots, x_s, x_{s+1}, \dots, x_{s+t}) \in (\mathbb{R}^n)^{s+t} \setminus \text{all diagonals} \mid \forall i \in \{1, \dots, s\}, x_i \in K\}.$$

Hence $C_{s,t}(K, \mathbb{R}^n)$ is the pullback of the following diagram:

$$\begin{array}{ccc} C_{s,t}(K, \mathbb{R}^n) & \longrightarrow & C_{s+t}(\mathbb{R}^n) \\ \downarrow & & \downarrow \text{restriction} \\ C_s(\mathbb{R}^j) & \xrightarrow{K^{\times s}} & C_s(\mathbb{R}^n) \end{array}$$

**Definition 2.28** (direction map) Let $\Gamma$ be a labeled BCR graph, $s = \#B(\Gamma)$ and $t = \#W(\Gamma)$. Let $e = (i, j)$ be an edge of $\Gamma$. Depending on if $e \in E_\theta(\Gamma)$ or $e \in E_\eta(\Gamma)$, the direction map $\phi_e = \phi_{ij}$ from $C_{s,t}(K, \mathbb{R}^n)$ to a sphere is defined as follows:

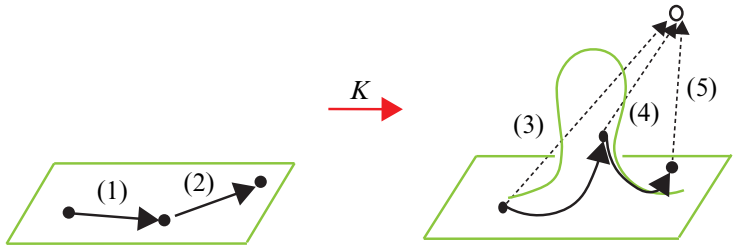


Figure 1: Graph and its direction maps.

- If $e=(i,j)\in E_\theta(\Gamma)$,
$$\phi_{ij}: C_{s,t}(K,\mathbb{R}^n)\to C_2(\mathbb{R}^n)=C_{0,2}(\varnothing,\mathbb{R}^n)\to S^{n-1}.$$
- If $e=(i,j)\in E_\eta(\Gamma)$,
$$\phi_{ij}: C_{s,t}(K,\mathbb{R}^n)\to C_2(\mathbb{R}^j)=C_{2,0}(K,\mathbb{R}^n)\to S^{j-1}.$$

In both cases, the first map is the restriction

$$(x_1,x_2,\dots,x_s,x_{s+1},\dots,x_{s+t})\mapsto(x_i,x_j),$$

and the second is defined as

$$(x,y)\mapsto\frac{y-x}{\|y-x\|}.$$

Intuitively, dashed edges measure the direction between two points in $\mathbb{R}^n$, while solid edges measure the direction in $\mathbb{R}^j$.

**Definition 2.29** (propagator) We define the differential form $\omega(K,\Gamma)$ on $C_{s,t}(K,\mathbb{R}^n)$ of degree $(n-1)\#E_\theta(\Gamma)+(j-1)\#E_\eta(\Gamma)$ by

$$\omega(K,\Gamma)=\bigwedge_{e\in E_\eta(\Gamma)}\phi_e^*\omega_{S^{j-1}}\bigwedge_{e\in E_\theta(\Gamma)}\phi_e^*\omega_{S^{n-1}}.$$

Here, the order of the wedge products is arbitrary, since both $\omega_{S^{j-1}}$ and $\omega_{S^{n-1}}$ are even forms when $n$ and $j$ are odd. We can use the order of edges, for example.

**Remark 2.30** The forms $\phi_e^*\omega_{S^{j-1}}$ and $\phi_e^*\omega_{S^{n-1}}$ are often called propagators. Leturcq [22] has given more flexible propagators to define invariants of embeddings into rational homology $n$-spheres.

The next proposition ensures the convergence of integrals we later define.

**Proposition 2.31** [4; 7, Proposition 1.2; 30] *There exists a canonical compactification $\overline{C}_{s,t}(K,\mathbb{R}^n)$ of $C_{s,t}(K,\mathbb{R}^n)$ such that $\phi_{ij}$ can be extended to the whole $\overline{C}_{s,t}(K,\mathbb{R}^n)$. The codimension 1 part of $\partial\overline{C}_{s,t}(K,\mathbb{R}^n)$ is*

$$\bigsqcup_{A\subset\{1,\dots,s,s+1,\dots,s+t,\infty\}}\widetilde{C}_A(K,\mathbb{R}^n),$$

*where $\widetilde{C}_A(K,\mathbb{R}^n)$ is "the configuration space with $A$ being infinitely close". (See Section 4.3 for details.)*

**Definition 2.32** We classify $\widetilde{C}_A(K,\mathbb{R}^n)$ ($A\subset\{1,\dots,s,s+1,\dots,s+t,\infty\}$ and $\#A\geq 2$) into four types as follows ($\Gamma_A$ is the subgraph of $\Gamma$ generated by vertices of $A$).

- **Infinite faces** $\infty\in A$.
- **Principal faces** $\#A=2$.
- **Hidden faces** $\#A\geq 3$ and $\Gamma_A$ is not the whole $\Gamma$; $\Gamma_A\subsetneq\Gamma$.
- **Anomalous faces** $\#A\geq 3$ and $\Gamma_A$ is the whole $\Gamma$; $\Gamma_A=\Gamma$.

**Notation 2.33** We write $E_{s,t}(\mathbb{R}^j,\mathbb{R}^n)$ for the bundle over $\mathrm{Emb}(\mathbb{R}^j,\mathbb{R}^n)$ whose fiber at a long embedding $K$ is the configuration space $C_{s,t}(K,\mathbb{R}^n)$. More precisely, $E_{s,t}(\mathbb{R}^j,\mathbb{R}^n)$ is the pullback of the following diagram:

$$\begin{array}{ccc} E_{s,t}(\mathbb{R}^j,\mathbb{R}^n) & \longrightarrow & C_{s+t}(\mathbb{R}^n) \\ \downarrow & & \downarrow{\scriptstyle \text{restriction}} \\ C_s(\mathbb{R}^j)\times\mathrm{Emb}(\mathbb{R}^j,\mathbb{R}^n) & \xrightarrow{\text{evaluation}} & C_s(\mathbb{R}^n) \end{array}$$

By abusing notation, we also write $E_{s,t}(\mathbb{R}^j,\mathbb{R}^n)$ for the bundle whose fiber is $\overline{C}_{s,t}(K,\mathbb{R}^n)$. We write $\widetilde{E}_A(\mathbb{R}^j,\mathbb{R}^n)$ for the bundle over $\mathrm{Emb}(\mathbb{R}^j,\mathbb{R}^n)$ whose fiber at a long embedding $K$ is the configuration space $\widetilde{C}_A(K,\mathbb{R}^n)$.

As in Definition 2.28, we can construct the direction map

$$\phi_e\colon E_{s,t}(\mathbb{R}^j,\mathbb{R}^n)\to S^{n-1}\quad\text{or}\quad \phi_e\colon E_{s,t}(\mathbb{R}^j,\mathbb{R}^n)\to S^{j-1}$$

depending on the type (solid or dashed) of $e$.

**Notation 2.34** We write $\omega(\Gamma)$ for the form on $E_{s,t}(\mathbb{R}^j,\mathbb{R}^n)$ defined by pulling back the standard volume forms $\omega_{S^{n-1}}$ and $\omega_{S^{j-1}}$ (in the same way as Definition 2.29).

**Definition 2.35** (configuration space integrals) Let $C_{s,t}$ (and $\overline{C}_{s,t}$) be a typical fiber of the bundle $\pi\colon E_{s,t}(\mathbb{R}^j,\mathbb{R}^n)\to\mathrm{Emb}(\mathbb{R}^j,\mathbb{R}^n)$. Let $\Gamma$ be a labeled BCR graph. We define the configuration space integral associated with $\Gamma$ by the fiber integral

$$I(\Gamma)=\int_{\overline{C}_{s,t}}\omega(\Gamma)=\int_{C_{s,t}}\omega(\Gamma).$$

The form $I(\Gamma)$ on $\mathrm{Emb}(\mathbb{R}^j,\mathbb{R}^n)$ is sometimes written as $\pi_*\omega(\Gamma)$.

By Stokes' theorem (see [7, Appendix] and [32, Appendix A.2]), we have

$$\begin{aligned} dI(\Gamma)&=\pi_*d\omega(\Gamma)+(-1)^r\pi_*^{\partial}\omega(\Gamma)\\ &=\int_{\overline{C}_{s,t}}d\omega(\Gamma)+(-1)^r\int_{\partial\overline{C}_{s,t}}\omega(\Gamma)=(-1)^r\int_{\partial\overline{C}_{s,t}}\omega(\Gamma)=(-1)^r\sum_A\int_{\widetilde{C}_A}\omega(\Gamma)\end{aligned}$$

where $r$ is the degree of $\int_{\partial \overline{C}_{s,t}} \omega(\Gamma)$. Hence for the closedness of $I(\Gamma)$, we should check that the integral over each $\widetilde{C}_A$ vanishes or is canceled.

Contributions of infinite faces vanish for dimensional reasons. (Recall that all our embeddings are standard outside a disk.)

**Theorem 2.36** [27, Theorem 5.10, Lemma 5.18] *If $\infty \in A$, the integral $\int_{\widetilde{C}_A} \omega(\Gamma)$ vanishes.*

On the other hand, contributions of principal faces are canceled when we sum up the configuration space integrals for graphs in a graph cocycle (with their coefficients).

**Theorem 2.37** [27, Theorem 5.11] *Let $\#A = 2$. The integral $\int_{\widetilde{C}_A} \omega(\Gamma)$ survives only when $A = e$ for some edge $e$ of $\Gamma$. Moreover,*

$$\int_{\widetilde{C}_e} \omega(\Gamma) = -\int_{C_{V(\Gamma/e)}} \omega(\delta_e \Gamma).^{3}$$

*Here $C_{V(\Gamma/e)}$ is the configuration space of vertices of $\Gamma/e$.*

## 3 Main result

Recall $r : \overline{\mathrm{Emb}}(\mathbb{R}^j, \mathbb{R}^n) \to \mathrm{Emb}(\mathbb{R}^j, \mathbb{R}^n)$ is the natural projection defined in Definition 2.4.

**Theorem 3.1** *Let $(n, j) = (\text{odd}, \text{odd})$ with $j \geq 3$.*

(1) *The linear combination of 2-loop BCR graphs of order 3*

$$H = \sum_{i=1}^{21} w(\Gamma_i)\Gamma_i$$

*is a graph cocycle. For the definition of $\Gamma_i$ and its coefficient $w(\Gamma_i)$, see Figure 2.*

(2) *Let $\bar{c}(H)$ be the correction term defined in Definition 4.6. Then*

$$\bar{z}_2^3 = r^* I(H) + \bar{c}(H) \in \Omega_{dR}^{3n-2j-7}\overline{\mathrm{Emb}}(\mathbb{R}^j, \mathbb{R}^n)$$

*is closed and $[\bar{z}_2^3] \in H_{dR}^{3n-2j-7}\overline{\mathrm{Emb}}(\mathbb{R}^j, \mathbb{R}^n)$ is nontrivial. In fact we can explicitly construct $\psi \in H_{3n-2j-7}\,\mathrm{Emb}(\mathbb{R}^j, \mathbb{R}^n)$ and its lift $\bar{\psi}$, so that the pairing $\bar{z}_2^3(\bar{\psi})$ is nontrivial. See Figure 10 for $\psi$, which is constructed from the presentation in Figure 13.*

(3) *Moreover, if $H_{dR}^{3n-j-6}(V_{n,j}(\mathbb{R})) = 0$, there is a nontrivial element $z_2^3 \in H_{dR}^{3n-2j-7}(\mathrm{Emb}(\mathbb{R}^j, \mathbb{R}^n))$. Here $V_{n,j} = V_{n,j}(\mathbb{R})$ is the real Stiefel manifold $\mathrm{SO}(n)/\mathrm{SO}(n-j)$.*

**Remark 3.2** [24, Theorem 3.14] When $(n, j) = (\text{odd}, \text{odd})$,

$$H_{dR}^*(V_{n,j}) \cong \bigwedge(e_{n-j}, e_{2(n-j)+3}, e_{2(n-j)+7}, \ldots, e_{2(n-j)+2j-3}).$$

In particular, if $j = 3$ then $H_{dR}^{3n-j-6}(V_{n,j}(\mathbb{R})) = 0$.

[3] We follow the inward normal convention for orientations of boundaries, which causes the sign of the right-hand side.

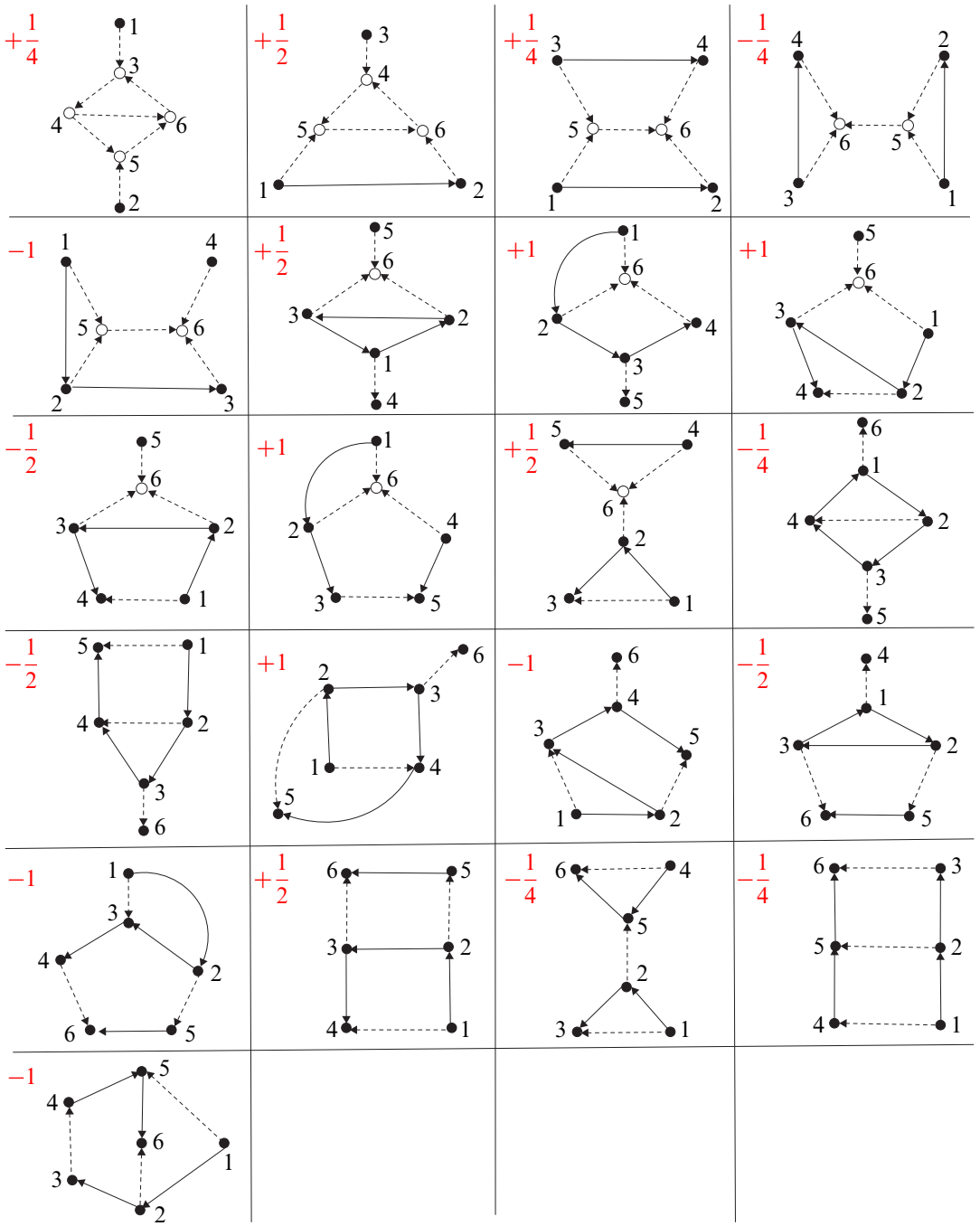


Figure 2: Nontrivial graph cocycle $H(\text{odd}, \text{odd})$.

**Remark 3.3** A similar graph to the first graph $\Gamma_1$ of Figure 2 appears in [3, Table C] as one of the rational homology generators of $\mathscr{E}^{m,n}$, the graph complex of hairy graphs. One can also check that $HH^{m,n}$ has the last graph as one of the rational generators.

We can take the above nontrivial cycle $\psi$ from the unknot component, and also over the 2-sphere when the codimension is 2.

**Corollary 3.4** $\pi_2(\mathrm{Emb}(\mathbb{R}^3, \mathbb{R}^5)_\iota) \otimes \mathbb{Q} \neq 0.$

# 4 Construction of the cocycles

In this section, we show $r^*I(H) + \bar{c}(H)$ is closed. According to the paragraphs after Definition 2.35, what to show is the vanishing of contributions of principal, hidden and anomalous faces.

## 4.1 H is a graph cocycle

We can show that $H$ is a graph cocycle, by direct computation of the coboundary map $\delta$ (defined in Definition 2.24). In this computation, we need to put together isomorphic graphs with different labels, taking their orientations into account. This will be the most difficult part when computing the graph cohomology through computer calculus.

Note that for the top degree, $\delta$ is described by a matrix (see Figure 3). We can easily see that the matrix is decomposed into blocks depending on the type of edges contracted:

(A) ○- - -○

(B) ●- - -●

(C) ○- - -●

(D) ●——●

## 4.2 Vanishing of contributions of hidden faces

Here, we show that contributions of hidden faces vanish. The fundamental approach is the following proposition. The cancellation using the symmetry as below was first introduced by Kontsevich [18]. Lescop gave a detailed explanation of it in [20; 21].

**Proposition 4.1** *Let $s = \#B(\Gamma)$, $t = \#W(\Gamma)$ and $\widetilde{C}_A \subset \partial C_{s,t}(K, \mathbb{R}^n)$ be a hidden face. If the subgraph $\Gamma_A$ of $\Gamma$ satisfies one of the following conditions, the contribution of the integral over $\widetilde{C}_A$ vanishes. (Below, $u$ and $b$ stand for univalent and bivalent, respectively.)*

(1) *$\Gamma_A$ is not connected.*

(2) *$\Gamma_A$ has a bivalent vertex of the following form (gray vertices can be both black and white):*

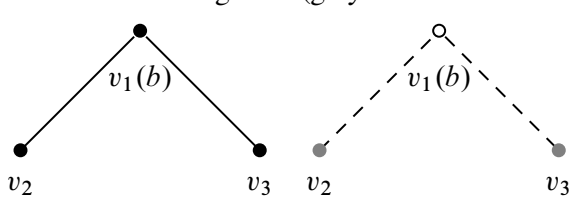

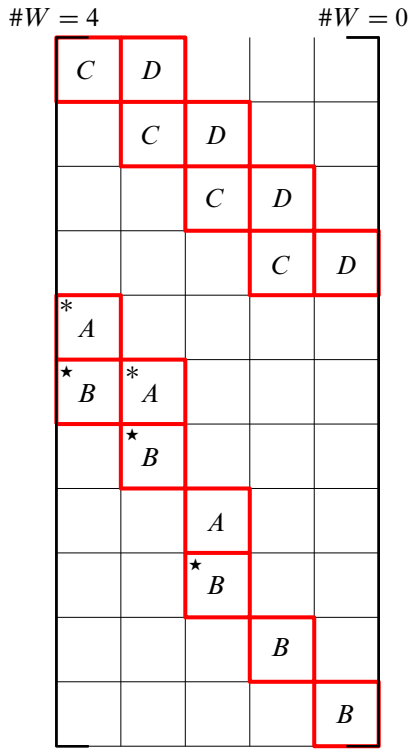


Figure 3: An example of the matrix of $\delta$. For our cocycle $H$, the blocks with $*$ are 0. The blocks with $\star$ do not appear.

(3) $\Gamma_A$ *has a univalent vertex of the following form*:

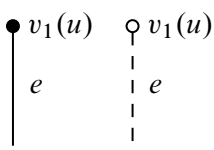


**Proof** For (2), we use the involution of $v_1$ with respect to the middle point of $v_2$ and $v_3$:

$$v_1 \mapsto v_2 + v_3 - v_1.$$

When $(n, j) = (\text{odd}, \text{odd})$, this involution reverses the orientation, while the integrand form does not change.

For (3), the group $\mathbb{R}_+$ acts on $\widetilde{C}_A$ by rescaling the edge $e$. Since the form $\omega(\Gamma)$ can be constructed through the projection

$$\widetilde{C}_A \to \widetilde{C}_A/\mathbb{R}_+,$$

where the quotient space on the right-hand side has less dimension, we can see the integral over $\widetilde{C}_A$ is zero.

For (1), we can use the action of $\mathbb{R}_+$ that increases or decreases the distance between two components. □

Unfortunately, our graph cocycle $H$ has hidden faces that satisfy none of the above conditions. However, since $(n, j) = (\text{odd}, \text{odd})$ we can apply the following proposition that was shown in [27].

**Proposition 4.2**
- *If $n - j =$ even and $\Gamma_A$ is a 0-loop (namely, $b_1(\Gamma_A) = 0$), the contribution of $\widetilde{C}_A$ vanishes.*
- *If $(n, j) = (\text{odd}, \text{odd})$ and $\Gamma_A$ is a 1-loop (namely, $b_1(\Gamma_A) = 1$), the contribution of $\widetilde{C}_A$ vanishes.*

**Remark 4.3** The second vanishing argument is also useful to cancel the contribution of the anomalous face, when $(n, j) = (\text{odd}, \text{odd})$ and the first Betti number of the graph is odd.

**Proof** The first statement is a consequence of similar involutions and rescaling to those of Proposition 4.1. We review the involution used to prove the second statement. This is an involution of all the vertices of $A$ with respect to one black vertex of $A$:

$$(x_1, x_2, \dots, x_s, x_{s+1}, x_{s+2}, \dots, x_{s+t}) \mapsto (x_1, 2x_1 - x_2, \dots, 2x_1 - x_s, 2\iota(x_1) - x_{s+1}, 2\iota(x_1) - x_{s+2}, \dots, 2\iota(x_1) - x_{s+t}).$$

Here, $\iota\colon \mathbb{R}^j \to \mathbb{R}^n$ is the linear injective map defined by the differential of the embedding. (If all the vertices of $A$ are white, take a white vertex as the central vertex $x_1$.) □

If a subgraph $\Gamma_A$ of $\Gamma_i$ in the cocycle $H$ is 2-loop, it satisfies one of (1), (2) or (3). Hence, it follows that all the contributions of hidden faces of $H$ do vanish.

## 4.3 Construction of correction terms for anomalous faces

We now proceed to construct a correction term to cancel the contribution of the integral over the anomalous face $\widetilde{C}_{V(\Gamma)}$. If $H^*_{dR}(V_{n,j}(\mathbb{R}))$ vanishes on a certain degree, we can construct a correction term $c$ as a form on $\mathrm{Emb}(\mathbb{R}^j, \mathbb{R}^n)$. Otherwise we construct one on $\overline{\mathrm{Emb}}(\mathbb{R}^j, \mathbb{R}^n)$, the space of long embeddings modulo immersions. Sakai in [27] follows the first approach, while Sakai and Watanabe do the second one in [29].

For the above purpose, we first describe the structure of each codimension one face $\widetilde{C}_A$. Readers can also refer to [6; 10; 27] for more detailed explanations. We only describe it when the subset $A \subset V(\Gamma) = \{1, \dots, s, s+1, \dots, s+t\}$ has at least one element of $\{1, \dots, s\}$. The anomalous face is the case where $A$ is equal to the entire $V(\Gamma)$.

The space $\widetilde{E}_A(\mathbb{R}^j, \mathbb{R}^n)$ is defined as the pullback of the following diagram. The configuration space $\widetilde{C}_A(K, \mathbb{R}^n)$ is the fiber of the projection $\widetilde{E}_A(\mathbb{R}^j, \mathbb{R}^n) \to \mathrm{Emb}(\mathbb{R}^j, \mathbb{R}^n)$ at an embedding $K$:

$$\begin{array}{ccc} \widetilde{E}_A(\mathbb{R}^j, \mathbb{R}^n) & \longrightarrow & B_A \\ \downarrow & & \downarrow b \\ E_{V/A}(\mathbb{R}^j, \mathbb{R}^n) & \xrightarrow{D} & \mathrm{Inj}(\mathbb{R}^j, \mathbb{R}^n) \\ \downarrow \pi & & \\ \mathrm{Emb}(\mathbb{R}^j, \mathbb{R}^n) & & \end{array}$$

Here, $\mathrm{Inj}(\mathbb{R}^j,\mathbb{R}^n)$ is the space of linear injective maps from $\mathbb{R}^j$ to $\mathbb{R}^n$. $E_{V/A}(\mathbb{R}^j,\mathbb{R}^n)$ is the bundle over $\mathrm{Emb}(\mathbb{R}^j,\mathbb{R}^n)$ whose fiber is the configuration space $C_{V/A}$ of $V(\Gamma)/A$. $B_A$ is the bundle over $\mathrm{Inj}(\mathbb{R}^j,\mathbb{R}^n)$ with the "normalized configuration space" of $A$ as the fiber; see Notation 4.4. $D$ is a map from $E_{V/A}(\mathbb{R}^j,\mathbb{R}^n)$ to $\mathrm{Inj}(\mathbb{R}^j,\mathbb{R}^n)$ which assigns the differential at the collapsed point $A/A$.

**Notation 4.4** We define the configuration spaces $C_{V/A}$ and $B_A$ as follows. Write $V(\Gamma)/A$ and $A$ as

$$V(\Gamma)/A=\{i_1,\dots,i_{s'},i_{s'+1},\dots,i_{s'+t'}\},$$
$$A=\{j_1,\dots,j_{s''},j_{s''+1},\dots,j_{s''+t''}\},$$

where $s'+s''=s+1$ and $t'+t''=t$. Then $C_{V/A}(K)$ for $K\in\mathrm{Emb}(\mathbb{R}^j,\mathbb{R}^n)$ and $B_A(I)$ for $I\in\mathrm{Inj}(\mathbb{R}^j,\mathbb{R}^n)$ are defined as

$$C_{V/A}(K)=C_{s',t'}(K),\quad B_A(I)=C_{s'',t''}(I)/\sim.$$

Here, $\sim$ is a relation generated by (a) rescalings (b) translations in the $I$ direction:

(a) $(x_{j_1},\dots,x_{j_{s''}},x_{j_{s''+1}},\dots,x_{j_{s''+t''}})\sim r(x_{j_1},\dots,x_{j_{s''}},x_{j_{s''+1}},\dots,x_{j_{s''+t''}})$, for $r\in\mathbb{R}_{>0}$;

(b) $(x_{j_1},\dots,x_{j_{s''}},x_{j_{s''+1}},\dots,x_{j_{s''+t''}})\sim v+(x_{j_1},\dots,x_{j_{s''}},x_{j_{s''+1}},\dots,x_{j_{s''+t''}})$, for $v/\!/I$.

Observe that if $A=V(\Gamma)$, (the restriction of) the form $\omega(\Gamma)$ on $\widetilde{E}_A(\mathbb{R}^j,\mathbb{R}^n)$ is described as the pullback of a form on $B_A$, for which we write $\omega(\Gamma)$, abusing notation.

Let $H=\sum_i\Gamma_i$ be a $g$-loop graph cocycle of order $k$. In the next proposition, we construct a correction term for anomalous faces when $H^d_{dR}(\mathrm{Inj}(\mathbb{R}^j,\mathbb{R}^n))=H^d_{dR}(V_{n,j})=0$ for a certain $d$.

**Proposition 4.5** *Assume that contributions of hidden faces of $H$ are canceled. For each $\Gamma$ of $H$, set $A=V(\Gamma)$ and consider the bundle $b\colon B_A\to\mathrm{Inj}(\mathbb{R}^j,\mathbb{R}^n)$. Then the fiber integral*

$$b_*\omega(H)=\sum_i b_*\omega(\Gamma_i)\in\Omega^d_{dR}(\mathrm{Inj}(\mathbb{R}^j,\mathbb{R}^n)),\quad d=k(n-j-2)+(g-1)(j-1)+(j+1),$$

*is closed. Moreover, when $b_*\omega(H)$ is exact, we can construct a correction term of the anomalous face by using $\mu\in\Omega^{d-1}_{dR}(\mathrm{Inj}(\mathbb{R}^j,\mathbb{R}^n))$ which satisfies $d\mu=(-1)^{r+1}b_*\omega(H)$, for $r=d-j$:*

$$c(H)=\pi_*D^*\mu.$$

**Proof** Without loss of generality, assume $H=\Gamma_1+\Gamma_2$. The first assertion follows because the integrals $b_{1*}\omega(\Gamma_1)$ and $b_{2*}\omega(\Gamma_1)$ do not have anomalous faces, while contributions of hidden and principal faces of the integrals are canceled.

Next, we show that $I(H)+c(H)$ is closed. Using Stokes' theorem (see the paragraph after Definition 2.35), we have

$$(-1)^r dI(H)=\int_{\widetilde{C}_{V(\Gamma_1)}}\omega(\Gamma_1)+\int_{\widetilde{C}_{V(\Gamma_2)}}\omega(\Gamma_2)=\pi_*D^*b_{1*}\omega(\Gamma_1)+\pi_*D^*b_{2*}\omega(\Gamma_2).$$

On the other hand,

$$(-1)^r dc(H) = (-1)^r d\pi_* D^*\mu = (-1)^r \pi_* D^* d\mu + \pi_*^{\partial} D^*\mu = -\pi_* D^* b_{1*}\omega(\Gamma_1) - \pi_* D^* b_{2*}\omega(\Gamma_2),$$

so $d(I(H) + c(H)) = 0$. □

Next, we consider the case $H^d_{dR}(\mathrm{Inj}(\mathbb{R}^j, \mathbb{R}^n)) = 0$ is not satisfied. In this case, we construct a correction term of

$$r^* I(H) \in \Omega^{k(n-j-2)+(g-1)(j-1)}\overline{\mathrm{Emb}}(\mathbb{R}^j, \mathbb{R}^n),$$

where $r : \overline{\mathrm{Emb}}(\mathbb{R}^j, \mathbb{R}^n) \to \mathrm{Emb}(\mathbb{R}^j, \mathbb{R}^n)$ is the natural projection defined in Definition 2.4. Define

$$\overline{D} : [0,1] \times C_1(\mathbb{R}^j) \times \overline{\mathrm{Emb}}(\mathbb{R}^j, \mathbb{R}^n) \to \mathrm{Inj}(\mathbb{R}^j, \mathbb{R}^n)$$

by $\overline{D}(t, x, \overline{K}) = D_x(\overline{K}_t)$, where $D$ is the differential. Note that $\overline{D}(1) = D \circ (\mathrm{id} \times r)$. Let

$$p_{23} : [0,1] \times C_1(\mathbb{R}^j) \times \overline{\mathrm{Emb}}(\mathbb{R}^j, \mathbb{R}^n) \to C_1(\mathbb{R}^j) \times \overline{\mathrm{Emb}}(\mathbb{R}^j, \mathbb{R}^n)$$

be the projection to the second and the third factors.

**Definition 4.6** We define the correction term for $\Gamma$ by

$$\bar{c}(\Gamma) = (-1)^r (-1)^{d+1} \pi_* p_{23*} \overline{D}^* b_* \omega(\Gamma).$$

For a graph cocycle $H = \sum_i \Gamma_i$, set $\bar{c}(H) = \sum_i \bar{c}(\Gamma_i)$.

**Proposition 4.7** *Let $H = \sum_i \Gamma_i$ be a graph cocycle such that contributions of hidden faces are canceled. Then $\bar{c}(H)$ is a correction term of $r^* I(H)$.*

**Proof** By using the closedness of $b_*\omega(H) = b_{1*}\omega(\Gamma_1) + b_{2*}\omega(\Gamma_2)$, we have

$$\begin{aligned}
(-1)^r d\bar{c}(H) &= (-1)^{d+1} \pi_* d(p_{23*} \overline{D}^* b_{1*}\omega(\Gamma_1)) + (-1)^{d+1} \pi_* d(p_{23*} \overline{D}^* b_{2*}\omega(\Gamma_2)) \\
&= -\pi_* (\mathrm{id} \times r)^* D^* b_{1*}\omega(\Gamma_1) - \pi_* (\mathrm{id} \times r)^* D^* b_{2*}\omega(\Gamma_2) \\
&= -r^* \pi_* D^* b_{1*}\omega(\Gamma_1) - r^* \pi_* D^* b_{2*}\omega(\Gamma_2) \\
&= -(-1)^r d(r^* I(H)).
\end{aligned}$$

See the diagram below:

$$\begin{array}{ccccc}
\mathrm{Emb}(\mathbb{R}^j, \mathbb{R}^n) & \xleftarrow[\pi]{} & C_1(\mathbb{R}^j) \times \mathrm{Emb}(\mathbb{R}^j, \mathbb{R}^n) & & \\
\uparrow{\scriptstyle r} & & \uparrow{\scriptstyle \mathrm{id}\times r} & \searrow^{D} & \\
\overline{\mathrm{Emb}}(\mathbb{R}^j, \mathbb{R}^n) & \xleftarrow[\pi]{} & C_1(\mathbb{R}^j) \times \overline{\mathrm{Emb}}(\mathbb{R}^j, \mathbb{R}^n) & & \mathrm{Inj}(\mathbb{R}^j, \mathbb{R}^n) \xleftarrow[b]{} B_{V(\Gamma)} \\
 & & \uparrow{\scriptstyle p_{23}} & \nearrow_{\overline{D}} & \\
 & & [0,1] \times C_1(\mathbb{R}^j) \times \overline{\mathrm{Emb}}(\mathbb{R}^j, \mathbb{R}^n) & &
\end{array}$$

□

# 5 Review of Sakai and Watanabe's construction of the wheel-like cycles

Here, we review Sakai and Watanabe's construction [29, Section 4] of the wheel-like cycles

$$c_k : (S^{n-j-2})^k \to \mathrm{Emb}(\mathbb{R}^j, \mathbb{R}^n), \quad \boldsymbol{v} \mapsto \varphi_k^{\boldsymbol{v}}$$

and

$$\tilde{c}_k : (S^{n-j-2})^k \to \overline{\mathrm{Emb}}(\mathbb{R}^j, \mathbb{R}^n)$$

for $k \geq 2$. The long embeddings $\varphi_k^{\boldsymbol{v}}$ are constructed by "perturbating" [29, 4.1.1] the original long embedding $\varphi_k$. The long embedding $\varphi_k$ is constructed from a specific oriented immersed 2-disk in $\mathbb{R}^3$, called the wheel-like ribbon presentation. This embedding $\varphi_k$ has specific $k$ parts called "crossings", where we can perform the perturbation to the direction $v_i \in S^{n-j-2}$ $(i = 1, \dots, k)$. This perturbation is analogous to the perturbation for constructing $k(n-3)$-cycles in $\mathrm{Emb}(\mathbb{R}^1, \mathbb{R}^n)$. (See [10].) These crossings can be described as images of several standard disks and annuli in $\mathbb{R}^j$ [29, 4.2.2], which look like "planetary systems". See [29, Figure 4.6].

Below, we often consider $\mathbb{R}^n$ as the product $\mathbb{R}^3 \times \mathbb{R}^{n-j-2} \times \mathbb{R}^{j-1}$. In this section, the standard embedding $\iota : \mathbb{R}^j \subset \mathbb{R}^n$ is considered as $x_1 \mapsto x_1$ and $x_i \mapsto x_{n-j+i}$ for $2 \leq i \leq j$.

## 5.1 The wheel-like ribbon presentations

The original embedding $\varphi_k$ is constructed from the wheel-like ribbon presentation $P \subset \mathbb{R}^3$ (defined below) by thickening $P$ and taking the boundary. The embedding $\varphi_k$ is realized in $\mathbb{R}^3 \times \mathbf{0} \times \mathbb{R}^{j-1}$.

**Definition 5.1** [29, Definition 4.1] The wheel-like ribbon presentation $P = \mathcal{D} \cup \mathcal{B}$ of order $k$ is a based oriented, immersed 2-disk in $\mathbb{R}^3$ such that

- $\mathcal{D} = D_0 \cup D_1 \cup \cdots \cup D_k$ are disjoint $(k+1)$ disks,
- $\mathcal{B} = B_1 \cup B_2 \cup \cdots \cup B_k$ are disjoint $k$ bands $(B_i \approx I \times I)$,
- $B_{i+1}$ connects $D_0$ with $D_i$ so that $B_{i+1} \cap D_0 = \{0\} \times I$ and $B_{i+1} \cap D_i = \{1\} \times I$ ($B_1$ is considered as $B_{k+1}$),
- $B_i$ intersects transversally with the interior of $D_i$,
- the base point $*$ is on the boundary of $D_0$ (but not on the boundaries of $B_i$).

Near the intersection of $B_i$ and $D_i$, they look, using a local coordinate, like

$$B = \{(x_1, x_2, x_3) \in \mathbb{R}^3 \mid |x_1| \leq \tfrac{1}{2}, |x_2| < 3, x_3 = 0\},$$
$$D = \{(x_1, x_2, x_3) \in \mathbb{R}^3 \mid |x_1|^2 + |x_3|^2 \leq 1, x_2 = 0\}.$$

See the left picture in Figure 4.

**Definition 5.2** [29, Definition 4.2] We define the ribbon $(j+1)$-disk $V_P$ by

$$V_P = \left(\mathcal{B} \times \left[-\tfrac{1}{4}, \tfrac{1}{4}\right]^{j-1}\right) \cup \left(\mathcal{D} \times \left[-\tfrac{1}{2}, \tfrac{1}{2}\right]^{j-1}\right) \subset \mathbb{R}^3 \times \mathbf{0} \times \mathbb{R}^{j-1}.$$

Note that the thicknesses of bands and that of disks are different.

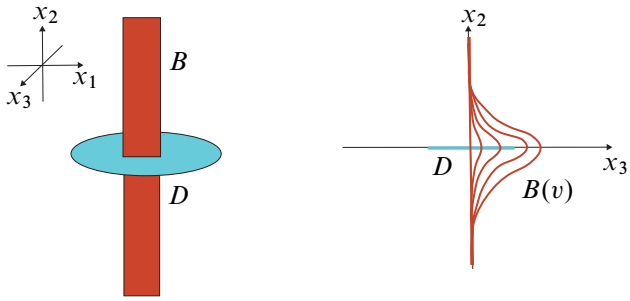


Figure 4: Perturbation of a crossing.

**Definition 5.3** After smoothing corners of $V_P$, the embedding $\varphi_k$ is defined by the connected sum $\partial V_P \# \iota(\mathbb{R}^j)$ at the base point.

## 5.2 Perturbation of crossings

Here, we define the perturbation $\varphi_k^{\boldsymbol{v}}$ of the original embedding $\varphi_k$. First, we define the perturbation $P_{\boldsymbol{v}}$ of the ribbon presentation $P$. The embedding $\varphi_k^{\boldsymbol{v}}$ is constructed from $P_{\boldsymbol{v}}$ in the same way as $\varphi_k$. Recall that the ribbon presentation $P$ is constructed in $\mathbb{R}^3 \times \mathbf{0} \times \mathbf{0}$, and the thickened presentation $V_p$ is constructed in $\mathbb{R}^3 \times \mathbf{0} \times \mathbb{R}^{j-1}$. The perturbation is performed using the coordinates $(x_4, \dots, x_{n-j+1})$ of $\mathbb{R}^{n-j-2}$ and the coordinate $x_3$ of $\mathbb{R}^3$.

**Notation 5.4** We consider the $(n-j-2)$-dimensional sphere $S^{n-j-2}$ as

$$S = S^{n-j-2} = \{(x_3, \dots, x_{n-j+1}) \in \mathbb{R}^{n-j-1} \mid (x_3-1)^2 + x_4^2 + \cdots + x_{n-j+1}^2 = 1\}.$$

Note that if $n-j-2=0$, $S$ is the set of two points $S^0 = \{x_3 = 0, x_3 = 2\}$.

**Notation 5.5** The band obtained by perturbing $B$ to the $v \in S$ direction is written as $B(v)$. (See the right picture in Figure 4)

$$B(v) = \{(x_1, x_2, \gamma(x_2)v) \in \mathbb{R}^2 \times \mathbb{R}^{n-j-1} \mid |x_1| \le \tfrac{1}{2}, |x_2| < 3\}.$$

Here $\gamma(y)$ is a test function defined as

$$\gamma(y) = \begin{cases} \exp\bigl(-y^2/\sqrt{9-y^2}\bigr) & \text{if } |y| \le 3, \\ 0 & \text{if } |y| \ge 3. \end{cases}$$

**Definition 5.6** We define $B_i(v_i)$, for $v_i \in S$, as the band in $\mathbb{R}^3 \times \mathbb{R}^{n-j-2}$ constructed from $B_i$ by replacing $B \times \mathbf{0}$ by $B(v_i)$. More precisely, let $U_i \subset \mathbb{R}^3 \times \mathbb{R}^{n-j-2}$ be a small neighborhood of the crossing $B_i \cap D_i$, and let

$$\xi_i : U_i \to [-3,3]^{n-j+1}$$

be a local coordinate that maps $B_i$ to $B \times \mathbf{0}$ and $D_i$ to $D \times \mathbf{0}$. Then $B_i(v_i)$ coincides with

$$(B_i \setminus U_i) \cup \xi_i^{-1}(B(v)).$$

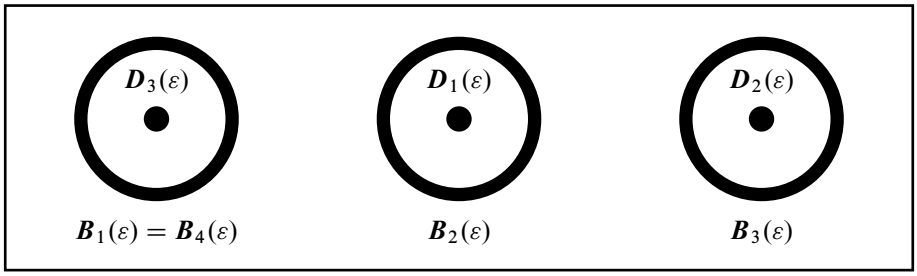


Figure 5: $\varphi_3^{\boldsymbol{v},\varepsilon}$ as embeddings from standard disks and annuli.

**Notation 5.7** Let $\boldsymbol{v} = (v_1, \dots, v_k) \in (S^{n-j-2})^k$. We define $\mathcal{B}_{\boldsymbol{v}}$ by

$$\mathcal{B}_{\boldsymbol{v}} = B_1(v_1) \cup B_2(v_2) \cup \cdots \cup B_k(v_k).$$

The perturbation $P_{\boldsymbol{v}} \subset \mathbb{R}^{n-j+1}$ of the wheel-like ribbon presentation $P$ is defined by $P_{\boldsymbol{v}} = \mathcal{D} \cup \mathcal{B}_{\boldsymbol{v}}$. Set

$$V_{P_{\boldsymbol{v}}} = \left(\mathcal{B}_{\boldsymbol{v}} \times \left[-\tfrac{1}{4}, \tfrac{1}{4}\right]^{j-1}\right) \cup \left(\mathcal{D} \times \left[-\tfrac{1}{2}, \tfrac{1}{2}\right]^{j-1}\right) \subset \mathbb{R}^n.$$

**Definition 5.8** As a submanifold in $\mathbb{R}^n$, the perturbation $\varphi_k^{\boldsymbol{v}}$ of $\varphi_k$ is defined by the connected sum $\partial V_{P_{\boldsymbol{v}}} \# \iota(\mathbb{R}^j)$. The parametrization of this submanifold is described in Section 5.3.

**Definition 5.9** We define the wheel-like cycle $c_k$ by

$$c_k : (S^{n-j-2})^k \to \mathrm{Emb}(\mathbb{R}^j, \mathbb{R}^n), \quad \boldsymbol{v} \mapsto \varphi_k^{\boldsymbol{v}}.$$

**Notation 5.10** [29, Definition 4.6] Let $\widehat{U}_i = U_i \times \left[-\frac{3}{4}, \frac{3}{4}\right]^{j-1}$. Inside the neighborhood $\widehat{U}_i$, there are two components $\widehat{D}_i$ and $\widehat{B}_i(v_i)$ of $\varphi_k^{\boldsymbol{v}}$. $\widehat{D}_i$ is homeomorphic to the punctured $j$-disk, while $\widehat{B}_i(v_i)$ is homeomorphic to the annulus $I \times S^{j-1}$. $\widehat{D}_i$ and $\widehat{B}_i(v_i)$ correspond to $D_i$ and $B_i(v_i)$ respectively. The pair $(\widehat{U}_i, \widehat{D}_i \cup \widehat{B}_i(v_i))$ is called the $i^{\text{th}}$ crossing of $\varphi_k^{\boldsymbol{v}}$.

## 5.3 The path to the trivial immersion

In the previous subsections, we have given a continuous $(S^{n-j-2})^{\times k}$-family of embedded $\mathbb{R}^j$ in $\mathbb{R}^n$. To give a parametrization to this submanifold $\varphi_k^{\boldsymbol{v}}$ for each $\boldsymbol{v}$, we consider sequential resolutions of crossings. (See [29, Remark 4,3].) These resolutions are possible in the space of immersions. More precisely, we consider a path from $\varphi_k^{\boldsymbol{v}}$ to the trivially immersed $\mathbb{R}^j$, associated with the following moves.

(m1) Pull the disk $D_i$ of each crossing to the $x_1$-direction so that $D_i$ and $B_i(v_i)$ do not intersect.

(m2) Pull back $D_i$ and $B_i(v_i)$ to the based disk $D_0$.

Using this path, we can equip each point of the submanifold $\varphi_k^{\boldsymbol{v}}$ with a coordinate. This parametrization is continuous with respect to $\boldsymbol{v}$. Moreover, this path gives a lift $\tilde{\varphi}_k^{\boldsymbol{v}}$ of $\varphi_k^{\boldsymbol{v}}$ to $\overline{\mathrm{Emb}}(\mathbb{R}^j, \mathbb{R}^n)$. We define the cycle $\tilde{c}_k : (S^{n-j-2})^k \to \overline{\mathrm{Emb}}(\mathbb{R}^j, \mathbb{R}^n)$ by $\boldsymbol{v} \mapsto \tilde{\varphi}_k^{\boldsymbol{v}}$.

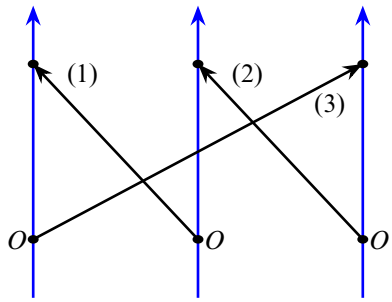


Figure 6: The cycle $c_3$ as a chord diagram on three directed lines.

### 5.4 Crossings as embeddings from standard disks and annuli

In [29], Sakai and Watanabe deformed $\varphi_k^{\boldsymbol{v}}$ by isotopy to give embeddings $\varphi_k^{\boldsymbol{v},\varepsilon}$. In this deformation, we "shrink" $\widehat{D}_i$ and $\widehat{B}_i(v_i)$ by $\varphi_k^{\boldsymbol{v}}$. See [29, 4.2.1] for the precise definition. This shrinking aims to make pairing arguments with cocycles easier. We write $\widehat{D}_i(\varepsilon)$ (resp. $\widehat{B}_i(v_i,\varepsilon)$) for the image of $\widehat{D}_i$ (resp. $\widehat{B}_i(v_i)$) by this deformation.

The $i^{\text{th}}$ crossing $(\widehat{U}_i, \widehat{D}_i(\varepsilon)\cup\widehat{B}_i(v_i,\varepsilon))$ of $\varphi_k^{\boldsymbol{v},\varepsilon}$ is described as an image of a standard disk and annulus $\boldsymbol{D}_i(\varepsilon)\cup\boldsymbol{B}_i(\varepsilon)$:

$$\boldsymbol{D}_i(\varepsilon) = \{(x_1,\dots,x_j)\in\mathbb{R}^j \mid (x_1-p_i)^2+x_2^2+\cdots+x_j^2\le(\varepsilon^2)^2\} \qquad (1\le i\le k),$$
$$\boldsymbol{B}_i(\varepsilon) = \{(x_1,\dots,x_j)\in\mathbb{R}^j \mid (3\varepsilon/4)^2\le(x_1-p_{i-1})^2+x_2^2+\cdots+x_j^2\le\varepsilon^2\} \quad (1\le i\le k+1),$$

where $p_i = i/k$ $(1\le i\le k-1)$ and $p_0 = p_k = 0$. Recall that $\boldsymbol{B}_1(\epsilon) = \boldsymbol{B}_{k+1}(\epsilon)$.

The subset $\bigcup_i \boldsymbol{D}_i\cup\bigcup_i \boldsymbol{B}_i(\varepsilon)$ looks like "planetary systems" on $\mathbb{R}^j$. (See Figure 5.)

**Remark 5.11** In Section 6, the cycle $c_k\colon \boldsymbol{v}\mapsto\varphi_k^{\boldsymbol{v},\varepsilon}$ is described as the chord diagram on $k$ directed lines as in Figure 6.

## 6 Construction of the cycles

In this section, we construct a cycle of the space of long embeddings from what we call "a set of planetary systems" on $\mathbb{R}^j$. Furthermore, we will see that such a set of planetary systems is described by a chord diagram on directed lines. The sets of planetary systems corresponding to Sakai and Watanabe's wheel-like cycles are the ones in which each planetary system has exactly one planetary orbit. (See Figure 5.) In terms of ribbon presentations, we use ribbon presentations with more than one node, while wheel-like ribbon presentations have exactly one node, the based disk $D_0$.

### 6.1 Planetary systems and chord diagrams on directed lines

Using the terminology "planetary system" for configuration spaces appears in Sinha's work [31].

**Definition 6.1** (a set of planetary systems on $\mathbb{R}^j$) A set of planetary systems $\mathcal{S}$ on $\mathbb{R}^j$ of order $k$ consists of the following:

(1) points $a_i$ at $(i, 0, \dots, 0) \in \mathbb{R}^j$ $(i = 1, \dots, s)$,

(2) spheres $S(L_i^l, a_i)$ $(l = 1, \dots, t_i)$ with radius $L_i^j$ centered at $a_i$ $(i = 1, \dots, s)$.

Here, $s$ and $t_i$ $(i = 1, \dots, s)$ are nonnegative integers such that the total number of points and spheres is $2k$.[4] We also assume $L_i^l$ is sufficiently smaller than 1, and assume $L_i^l$ is sufficiently smaller than $L_i^{l'}$ if $l < l'$. For example, set $\delta = 1/10^N$ and $L_i^l = \delta^{(t_i+1-l)}$.

Below we call points of (1) fixed stars. We call spheres of (2) planetary orbits. Each fixed star forms one planetary system which consists of $t_i$ planetary orbits.

**Definition 6.2** An ordered pairing $\{p_i\}_{i=1,\dots,k}$ for $\mathcal{S}$ is a pairing among the set of fixed stars and planetary orbits. Fixed stars must be paired with planetary orbits. Planetary orbits may be paired with other planetary orbits (orbit-orbit pairing). The order of two elements of each pair is taken so that the fixed star (if it exists) is the first.

A set of planetary systems and its ordered pairing can be described by a chord diagram on directed lines.

**Definition 6.3** (chord diagram on directed lines) A chord diagram on $s$ directed lines of order $k$ consists of the following data.

- Integers $t_i \geq 0$ $(i = 1, \dots, s)$ such that
$$\sum_{i=1}^{s} (t_i + 1) = 2k.$$
- An ordered pairing $\{p_i\}_{i=1,\dots,k}$ among $2k$ points $V = \{(i, l) \in \mathbb{Z}^2 | 1 \leq i \leq s, 0 \leq l \leq t_i\}$.

Such a chord diagram is drawn as:

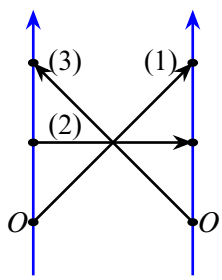


The ordered pairing must be taken so that it satisfies:

- At least one of the two points of each pair is not on the $x$-axis (that is, its second coordinate is not zero).
- Any point $v = (i, 0)$ on the $x$-axis must be the first of some ordered pair.

[4] $s$ and $t_i$ here are not related to $s$ and $t$ of $C_{s,t}$.

A set of planetary systems and its ordered pairing determines a chord diagram on directed lines in an expected way. Namely, points on the $x$-axis are fixed stars. Other points are planetary orbits. Conversely, a chord diagram on directed lines determines a set of planetary systems (up to rescalings) and its ordered pairing.

Let $C$ be a chord diagram on directed lines. Remember that the set of chords (pairings) $E(C)$ is ordered, and each chord is oriented.

**Definition 6.4** (induced ordering of $V(C)$) We order the set of vertices $V(C)$ in a canonical way using the above ordering and orientations. That is, the initial vertex of the $i^{\text{th}}$ chord is labeled by $(2i-1)$. The end vertex of the $i^{\text{th}}$ chord is labeled by $2i$.

Using the ordering of $V(C)$, let the image of $\tau\colon\{1,\dots,g-1\}\to\{1,\dots,2k\}=V(C)$ be the first vertices of orbit-orbit pairing; $g=k-s$. We assume that $\tau$ preserves the orders.

## 6.2 Construction of the cycles

Once we fix a set of planetary systems and its ordered pairing, namely a chord diagram on directed lines, we can construct a "generalized ribbon cycle". These generalized cycles have more parameters than the wheel-like cycles in Section 5.

**Definition 6.5** (generalized ribbon cycles) Let $\mathcal{S}$ be a set of planetary systems of order $k$. Let $\{p_i\}_{i=1,\dots,k}$ be an ordered pairing. Let $(g-1)$ be the number of orbit-orbit pairings. From this data, we construct a $k(n-j-2)+(g-1)(j-1)$ cycle $\psi=\psi(\mathcal{S},\{p_i\}_{i=1,\dots,k})$ in the following. We call this cycle the generalized ribbon cycle associated with $(\mathcal{S},\{p_i\}_{i=1,\dots,k})$. For simplicity, we only construct for the following case:

- There is only one fixed star $a_1$ (and hence one planetary system).
- There are three planetary orbits $S(L_l,a_1)$ for $l=1,2,3$.
- The pairing is taken as $(a_1,S(L_2))$, $(S(L_1),S(L_3))$.

The corresponding chord diagram is

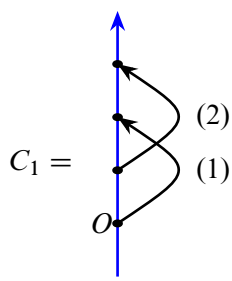


The cycles corresponding to other $(\mathcal{S},\{p_i\}_{i=1,\dots,k})$ are constructed similarly.

Below we construct a cycle in $\mathrm{Emb}(\mathbb{R}^j,\mathbb{R}^n)$,

$$\phi\colon S^{j-1}\times S^{n-j-2}\times S^{n-j-2}\to\mathrm{Emb}(\mathbb{R}^j,\mathbb{R}^n).$$

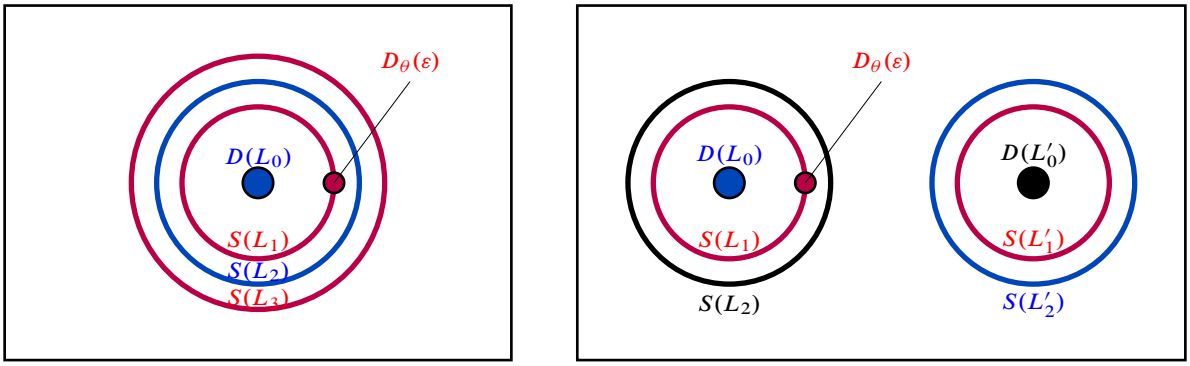


Figure 7: Preimage on $\mathbb{R}^j$ of $\phi$ (left) and $\psi$ (right).

Let $S(L)$ and $D(L)$ denote the $(j-1)$-sphere and $j$-ball respectively, of radius $L$ centered at $O$ in $\mathbb{R}^j$. And let $L_0, L_1, L_2, L_3 \in \mathbb{R}$ satisfy

$$0 < L_0 < L_1 < L_2 < L_3 < L_4 = 1,$$

where $L_i$ is sufficiently smaller than $L_{i+1}$ (for example, set $L_i = \delta^{4-i}$). For each $\theta \in S^{j-1}$, we write $D_\theta(\varepsilon)$ for the ball of radius $\varepsilon$ centered at $\theta \in S(L_1)$. We assume $\varepsilon$ is sufficiently smaller than $L_1$. (See Figure 7.) Steps 1 and 2 below are to construct a cycle $\phi_\theta \colon S^{n-j-2} \times S^{n-j-2} \to \mathrm{Emb}(\mathbb{R}^j, \mathbb{R}^n)$ for each parameter $\theta \in S^{j-1}$. Let $0 < h_4 < h_3 < h_2 < h_1 < h_0$ be coordinates of the $x_{j+1}$ axis.

**Step 1** Deform $D(L_3)$ by isotopy in $\mathbb{R}^j \times \mathbb{R} \subset \mathbb{R}^n$ to the $x_{j+1}$ direction, so that $\mathbb{R}^j$ is embedded in $\mathbb{R}^{j+1}$ as

$$S(r) \times (h_4, h_0)$$

in the range $h_4 < x_{j+1} < h_0$. Here $S(L_3)$, $S(L_2)$ and $S(L_1)$ are mapped to $S(r) \times \{h_3\}$, $S(r) \times \{h_2\}$ and $S(r) \times \{h_1\}$ respectively. We assume $r$ is sufficiently small compared to $\min\{|h_i - h_{i+1}|\}_i$.

**Step 2** For $L = L_2, L_3$, let $S(L) \times I$ be the tubular neighborhood of $S(L)$ in $\mathbb{R}^j$ with width $2\varepsilon$. Construct a ribbon crossing of $S(L_3) \times I$ and $D_\theta(\varepsilon)$ near $S(r) \times h_3$, and a ribbon crossing of $S(L_2) \times I$ and $D(L_0)$ near $S(r) \times h_2$. Here, a ribbon crossing is the crossing given by the perturbation of a crossing of a ribbon presentation as in Section 5.2. See Figure 8. Then we obtain a cycle

$$\phi_\theta \colon S^{n-j-2} \times S^{n-j-2} \to \mathrm{Emb}(\mathbb{R}^j, \mathbb{R}^n).$$

We describe a ribbon presentation corresponding the cycle $\phi_\theta$ in Section 6.3. By choosing a ribbon presentation suitably, we can construct this cycle in the unknot component.

**Step 3** Move $D_\theta(\varepsilon)$ on $S(L_1)$. In $\mathbb{R}^{j+1}$, we change the behavior only near $h_1$. At the height $h_1$, we turn the branch tube around the stem tube. See Figure 8. Then we get the desired cycle $\phi$. The parametrization of $\phi$ is given in Section 6.4.

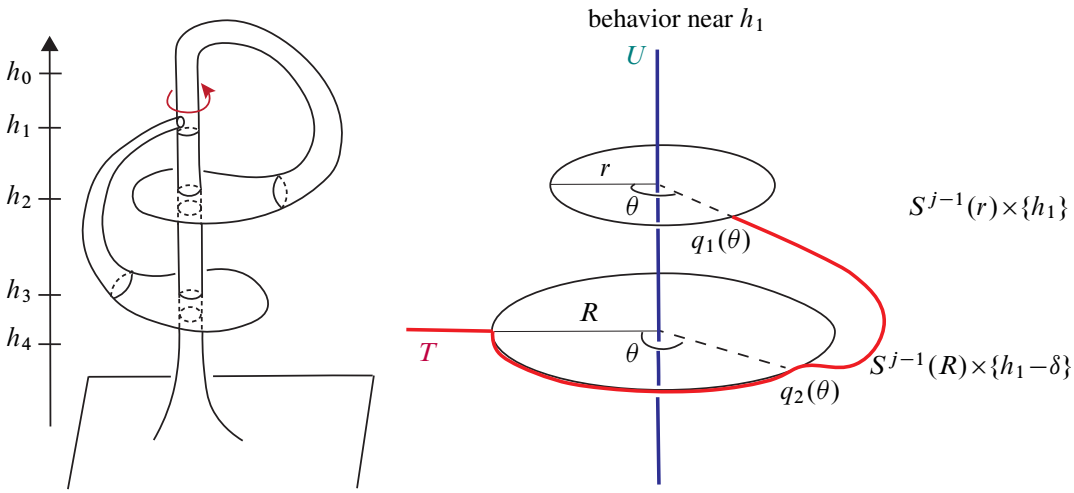


Figure 8: Image on $\mathbb{R}^{j+1}$.

We describe Step 3 more precisely. We write $U$ for the stem tube $S^{j-1}(r)\times(h_4,h_0)$. In Figure 8, we draw the core $c_U$ of $U$ in blue. For $\theta\in S^{j-1}$, let $\partial D_\theta(\varepsilon)$ be mapped to the $\theta$ side of $U$. For the initial point $O=(1,0,\dots,0)\in S^{j-1}$, we construct, near $h_1$, a branch tube $T=T(O)$ with small radius which starts from $U$ and goes to the $x_1$-direction. We draw the core $c=c(O)$ of $T$ in red.

For $\theta\in S^{j-1}$, we replace the core $c$ with $c(\theta)$ defined as follows.

- $c(\theta)$ starts from the point $q_1(\theta)=(r\theta,h_1)\in S^{j-1}(r)\times\{h_1\}$ and goes straight to the point $(R\theta,h_1)\in S^{j-1}(R)\times\{h_1\}(R>r)$.
- Next, $c(\theta)$ runs down to $S^{j-1}(R)\times\{h_1-\delta\}$ preserving $\theta\in S^{j-1}(R)$ and reaches the point $q_2(\theta)=(R\theta,h_1-\delta)$.
- Then $c(\theta)$ connects $q_2(\theta)$ and $q_2(O)$ through the shortest geodesic of $S^{j-1}(R)$.

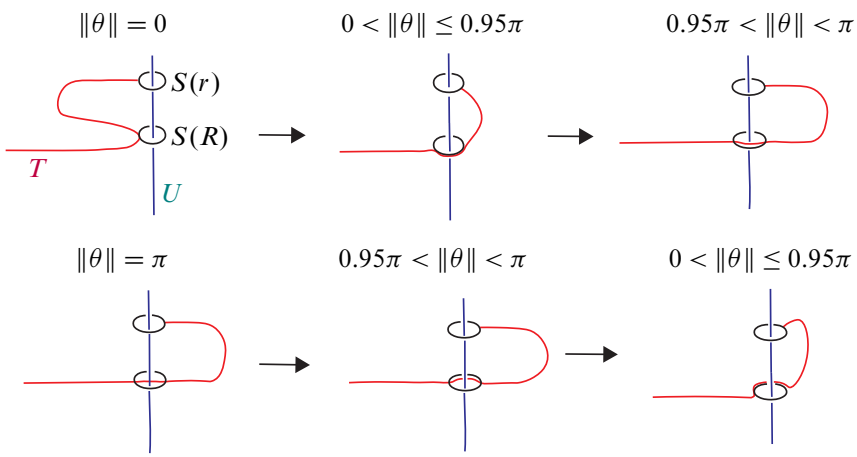


Figure 9: The replaced core $c(\theta)$ near $h_1$ ($a=0.05\pi$).

However, there is one problem. When $\theta$ is the antipode $A \in S^{j-1}$ of the base point $O$, there are infinitely many geodesics from $q_2(A)$ to $q_2(O)$. To avoid this, $c(\theta)$ takes a short-cut from $q_2(\theta)$ to $q_2(O)$ inside the ball $D^j(R)$, when $\theta$ is in a small neighborhood of $A$. At the same time, when $\theta$ is near $A$, we perturb $c(\theta)$ to the $x_{j+2}$-direction.

More precisely, let

$$\|\cdot\|\colon S^{j-1} \to [0,\pi]$$

be the function that assigns the geodesic distance from the base point $O$. Then in the range $\|\theta\| > \pi - a$ for a sufficiently small $a$, we assume that the core $c(\theta)$ approaches the core $c_U$ of $U$, and assume that they intersect with each other in $\mathbb{R}^{j+1}$ when $\|\theta\| = \pi$. At this time, we perturb $c(\theta)$ in the positive direction of the $x_{j+2}$ axis. See Figure 9.

Then we take a tubular neighborhood $N(\theta) \in \mathbb{R}^{j+1}$, which is perturbed to the $x_{j+2}$ direction when $\|\theta\| > \pi - a$. The replaced tube $T(\theta)$ is defined as the boundary of $N(\theta)$.

As a candidate of a dual cycle of $H$, we construct the generalized ribbon cycle in Figure 10 from the diagram

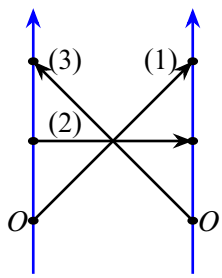


The ribbon presentation corresponding to the cycle $\psi$ is given in Section 6.3. The cycle $\psi$ is also constructed in the unknot component. In general, cycles have parameters $\theta_i' \in S^{j-1}$ $(i = 1,\dots,g-1)$ and $y_j \in S^{n-j-2}$ $(j = 1,\dots,k)$.[5]

## 6.3 Ribbon presentations with more than one node

Here, we give ribbon presentations corresponding to the (cycles of) long embeddings in Section 6.2. (We review the notation of ribbon presentations at the beginning of this subsection.) These ribbon presentations have a node other than the based disk $D_0$, and this node is connected (by two bands) to two leaves. Using moves of ribbon presentations, we show that the cycles of Section 6.2 are in the path component of the trivial long embedding. The key point is the way the two leaves intersect with bands.

**Definition 6.6** A ribbon presentation $P = \mathcal{D} \cup \mathcal{B}$ of order $k$ is a based oriented, immersed 2-disk in $\mathbb{R}^3$ such that

- $\mathcal{D} = D_0 \cup D_1 \cup \cdots \cup D_k$ are disjoint $(k+1)$ disks,

[5]We change the notation for the parameter moving on $S^{j-1}$, from "$\theta$" to "$\theta'$". In Section 7, we use the letter "$\theta$" for a different parameter.

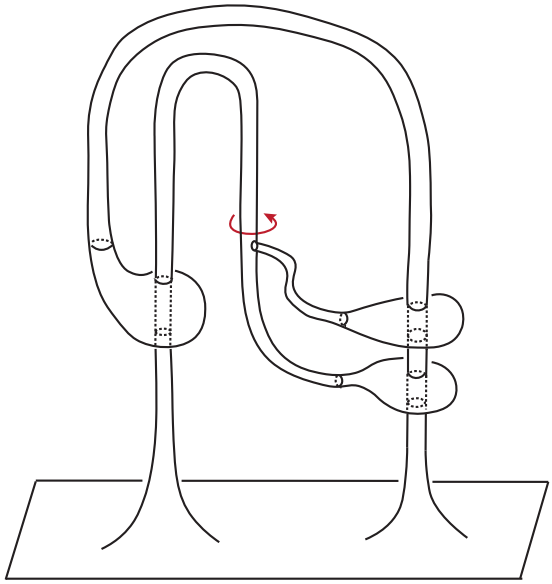

Figure 10: The cycle $\psi$.

- $\mathcal{B} = B_1 \cup B_2 \cup \cdots \cup B_k$ are disjoint $k$ bands ($B_i \approx I \times I$),
- each band connects two different disks,
- $B_i$ can intersect transversally with the interior of disks,
- the base point $*$ is on the boundary of $D_0$ (but not on the boundaries of $B_i$).

**Notation 6.7** [17, Definition 3.1] A disk without intersecting bands is called a node. A disk is called a leaf if it has at least one intersecting band and it is incident to exactly one band. We draw a gray disk for a node except for the based disk $D_0$. We call a ribbon presentation simple if each leaf intersects with exactly one band.

In [17], Habiro and Shima introduced moves of ribbon presentations that do not change the isotopy class of the ribbon 2-knot represented by the presentation. The following are examples of the moves.

**Notation 6.8** We define $S1$ and $S4$ moves as in Figure 11.

To the chord diagrams

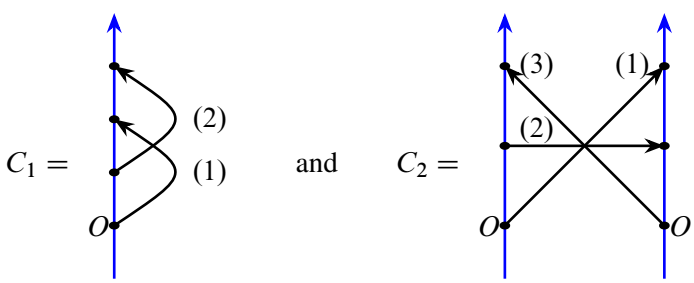

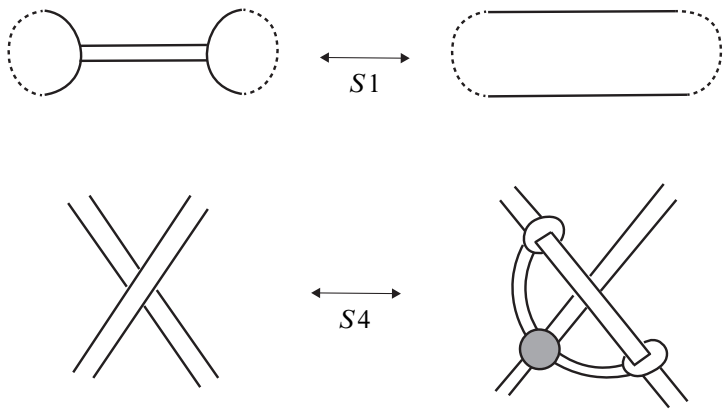


Figure 11: $S1$ and $S4$ moves.

we assign the simple ribbon presentations $P_1$ in Figure 12 and $P_2$ in Figure 13. Each directed line corresponds to a sequence of bands and nodes that connects the based disk $D_0$ and a leaf. The origin of each directed line corresponds to this leaf. Each chord corresponds to a crossing. The initial point of each chord corresponds to the disk (leaf) of the crossing. If this initial point is not an origin, this leaf is connected to a node by a band. The target point of each chord corresponds to a small segment of the band of the crossing.

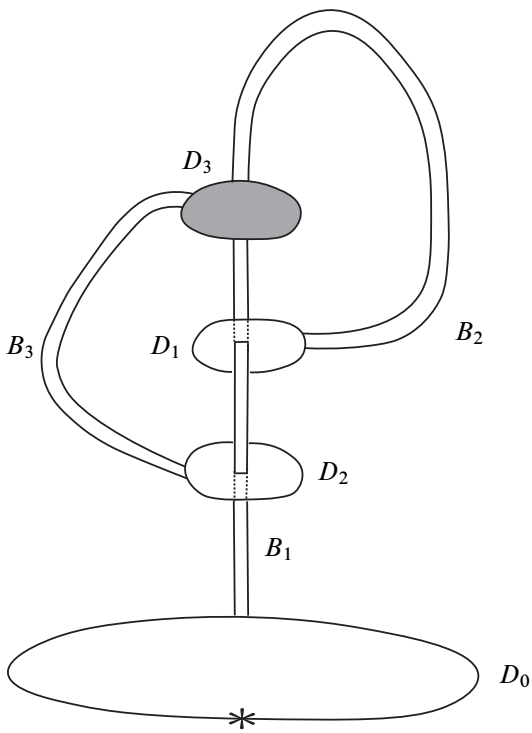


Figure 12: Ribbon presentation $P_1$ corresponding to $C_1$.

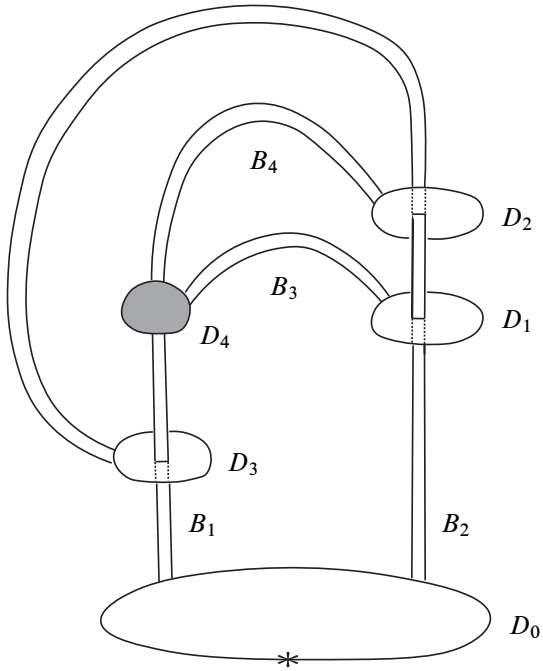


Figure 13: Ribbon presentation $P_2$ corresponding to $C_2$.

Observe that our chord diagrams $C_1$ and $C_2$ have a subdiagram of the form

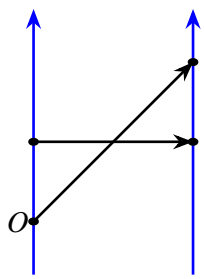


Recall that we have constructed a crossing for each chord. There are two ways to construct a crossing, depending on which orientation the band intersects with the disk. In the part

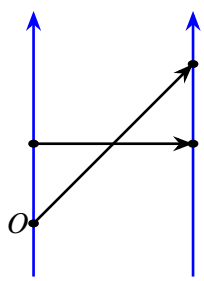


we choose the left presentation of Figure 14. That is, we assume that two crossings have opposite orientations. We can write this crossing information on chord diagrams by assigning a sign to each chord.

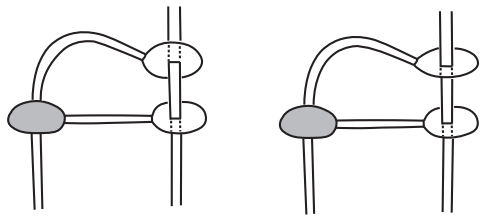

Figure 14: Suitable ribbon presentation (left).

For $C_1$ and $C_2$, we choose

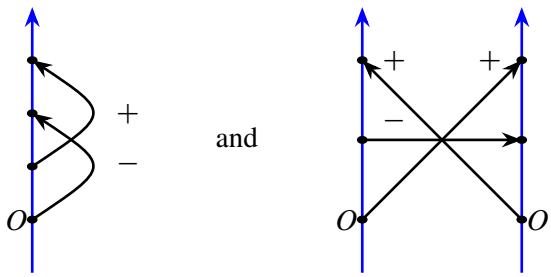


**Notation 6.9** Let $\phi$ and $\psi$ be the cycles constructed from the ribbon presentations $P_1$ and $P_2$ in Section 6.2. If $n-j=2$, define the cycle

$$\psi(0,0,0)\colon S^{j-1} \to \overline{\mathrm{Emb}}(\mathbb{R}^j, \mathbb{R}^{j+2})$$

as the $(0,0,0) \in S^0 \times S^0 \times S^0$ component of $\psi$, that is, the component where no crossing is resolved. Define $\phi(0,0)$ similarly.

**Proposition 6.10** *The ribbon presentations $P_1$ and $P_2$ are equivalent to the trivial presentation. Thus, when $n-j \geq 3$, both $\phi$ and $\psi$ are in the unknot component. When $n-j=2$, both $\phi(0,0)$ and $\psi(0,0,0)$ are in the unknot component.*

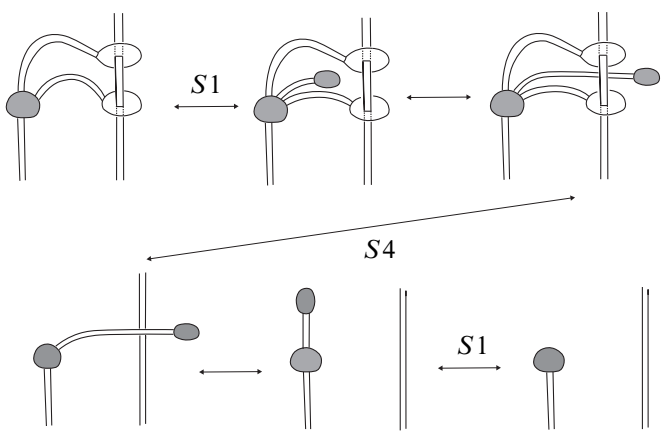


Figure 15: Resolving the pair of two crossings.

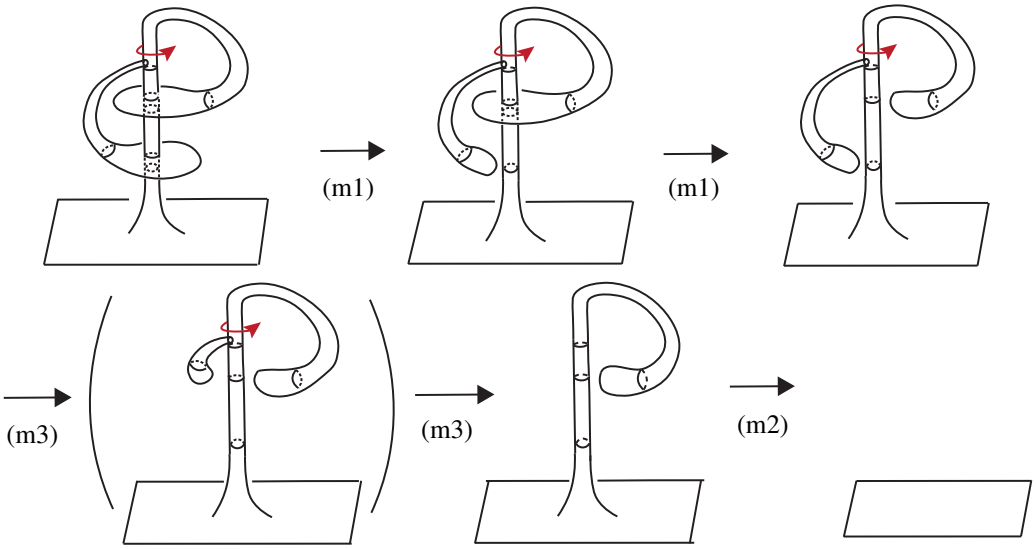


Figure 16: Lift of $\phi$ to $\overline{\mathrm{Emb}}(\mathbb{R}^j, \mathbb{R}^n)$.

**Proof** By using moves of ribbon presentations including $S4$, we can resolve the pair of two crossings of opposite orientations as in Figure 15. Then, we can show the resulting ribbon presentation is equivalent to the trivial presentation. □

### 6.4 Lifting the cycles to $\overline{\mathrm{Emb}}(\mathbb{R}^j, \mathbb{R}^n)$

Finally, we give a parametrization to the cycle $\phi$ and the cycle $\psi$ respectively. We give this parametrization by using a path to the trivially immersed $\mathbb{R}^j$ as in Section 5.3. Moreover, this path gives a lift of $\phi$ and $\psi$ to $\overline{\mathrm{Emb}}(\mathbb{R}^j, \mathbb{R}^n)$.

The path is constructed as follows. Let $\widehat{D}_i$ be the ball of crossings corresponding to $D_\theta(\varepsilon)$. In the ribbon presentation, the disk $D_i$ is connected to the node. First, we resolve each crossing, by the move (m1) of Section 5.3. Then

(m3) pull back $\widehat{D}_i$ to the stem tube (see Figure 16).

Finally, we deform the immersion to the trivial immersion by the move (m2) of Section 5.3.

## 7 Some lemmas for computing cocycle-cycle pairing

In this section, we state preliminary lemmas which are used to calculate pairings between cocycles and cycles of the space of long embeddings, as pairings between graphs and diagrams (see Theorem 7.14). Readers who are familiar with configuration space integrals may skip until Lemma 7.7. Graphs in this section are admissible (see Definition 2.19) graphs of defect 0.

## 7.1 Preliminary lemmas

**Lemma 7.1** (symmetry lemma) *Let a labeled BCR graph $\Gamma$ have an even symmetry $\iota$ (a change of labels of even sign that produces the same labeled graph). Consider the involution on $C_{s,t}$*

$$\sigma : (x_1, x_2, \dots, x_s, x_{s+1}, \dots, x_{s+t}) \mapsto (x_{\iota^{-1}(1)}, x_{\iota^{-1}(2)}, x_{\iota^{-1}(s)}, x_{\iota^{-1}(s+1)}, \dots, x_{\iota^{-1}(s+t)}).$$

*Let the two disjoint submanifolds $X$ and $Y$ of $C_{s,t}$ satisfy $\sigma(X) = Y$. Then $\int_X I(\Gamma) = \int_Y I(\Gamma)$.*

**Proof** We observe that

$$\int_Y I(\Gamma) = \int_{\sigma(X)} (\sigma^{-1})^* I(\Gamma),$$

since the changes of signs are canceled. □

**Lemma 7.2** (localizing lemma [29, Lemma 4.7]) *Let $\Gamma$ be a BCR graph of order $k$, $\#B(\Gamma) = s$ and $\#W(\Gamma) = t$. Let $\psi$ be a generalized ribbon cycle with crossings $p_1, \dots, p_k$. Recall that each crossing consists of the image of a ball $D_{p_i}$ (or $D_{p_i}(\theta'^{-1}_{\tau^{-1}(2i-1)})$) and the image of an annulus $I \times S_{p_i}$. Let $C_0$ be the subspace of $C_{s,t}(\psi)$ which consists of configurations $(x_1, x_2, \dots, x_s, x_{s+1}, \dots, x_{s+t})$ satisfying the following:*

- *There exists $i$ such that either $D_{p_i}$ or $I \times S_{p_i}$ has no black vertex.*

*Then $\int_{C_0} I(\Gamma) = 0$.*

**Proof** Let $p_i$ be such a crossing. Then the contribution of the integral vanishes by dimensional reasons (or is canceled) with respect to the parameter $y_i$ of the crossing $p_i$. □

Set

$$X_\alpha = \begin{cases} D_{p_i} \text{ or } D_{p_i}(\theta'^{-1}_{\tau^{-1}(2i-1)}) & \text{if } \alpha = 2i-1, \\ I \times S_{p_i} & \text{if } \alpha = 2i. \end{cases}$$

By the localizing lemma, we only consider the graph with $s = 2k$ and $t = 0$, and configurations that there are some black vertex $x_{\sigma^{-1}(\alpha)}$ in $X_\alpha$. We write the set of these configurations as $C_\sigma$, $\sigma \in \mathfrak{S}_{2\alpha}$. If $\sigma \neq \tau$, $C_\sigma$ and $C_\tau$ have no intersection.

**Lemma 7.3** (pairing lemma [29, Lemma 4.9]) *If $x_{\sigma^{-1}(2i-1)} \in D_{p_i}$ and $x_{\sigma^{-1}(2i)} \in I \times S_{p_i}$ are not connected by dashed edges, $\int_{C_\sigma} I(\Gamma) = 0$.*

**Proof** This can be shown by a similar dimensional reason to the proof of Lemma 7.2. □

**Lemma 7.4** (same system lemma [29, Lemma 4.8]) *Let $\Gamma$ be a BCR graph of order $k$ (and defect 0), $\#B(\Gamma) = 2k$ and $\#W(\Gamma) = 0$. Let $\psi$ be a generalized ribbon cycle with crossings $p_1, \dots, p_k$. If $X_\alpha$ and $X_\beta$ are in different planetary systems, and $x_{\sigma^{-1}(\alpha)}$ and $x_{\sigma^{-1}(\beta)}$ are connected by solid edges (see Figure 17), $\int_{C_\sigma} I(\Gamma) = 0$.*

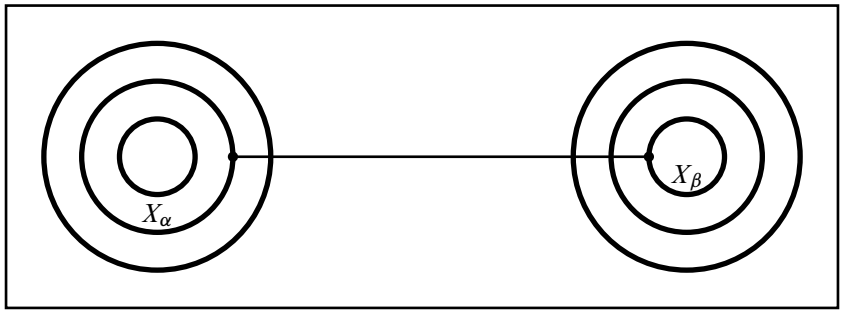


Figure 17: An edge connecting different systems.

**Proof** This is because the direction

$$\frac{x_{\sigma^{-1}(\beta)} - x_{\sigma^{-1}(\alpha)}}{\|x_{\sigma^{-1}(\beta)} - x_{\sigma^{-1}(\alpha)}\|} \in S^{j-1}$$

varies in a small neighborhood of a point in $S^{j-1}$. □

**Remark 7.5** More precisely, $\int_{C_\sigma} I(\Gamma) = 0$ above means $\int_{C_\sigma} I(\Gamma)$ approaches 0 as the radii of the two planetary systems approach 0.

**Lemma 7.6** (ingoing lemma) *Let $\Gamma$ be a BCR graph of order $k$, $\#B(\Gamma) = 2k$ and $\#W(\Gamma) = 0$. Let $\psi$ be a generalized ribbon cycle with crossings (pairings) $p_1, \dots, p_k$. Let $X_\alpha$ be a planetary orbit in a planetary system. Assume that all solid edges adjacent to $x_{\sigma^{-1}(\alpha)}$ are outgoing. That is, if $x_{\sigma^{-1}(\alpha)}$ and $x_{\sigma^{-1}(\beta)}$ are connected by solid edges, $X_\beta$ is outside $X_\alpha$ (see Figure 18). Then $\int_{C_\sigma} I(\Gamma) = 0$.*

**Proof** Since the integrand form does not depend on the parameter $x_{\sigma^{-1}(\alpha)}$, it factors through

$$C_\sigma \to C_\sigma / X_\alpha.$$

□

**Lemma 7.7** (decomposing lemma)

- *Let $e = \{\sigma^{-1}(\alpha), \sigma^{-1}(\beta)\}$ be a solid edge. Let $X_\alpha$ and $X_\beta$ be in the same planetary system and $X_\beta$ be outside. Then if $X_\beta = I \times S_p$, $\phi_e^* \omega_{S^{j-1}}$ depends only on the variable $\theta_{\sigma^{-1}(\beta)} \in S_p$ of $x_{\sigma^{-1}(\beta)} = (r_{\sigma^{-1}(\beta)}, \theta_{\sigma^{-1}(\beta)}) \in X_\beta$. If $X_\beta = D_p(\theta')$, it depends only on $\theta'$.*
- *Let $e = \{\sigma^{-1}(\alpha), \sigma^{-1}(\beta)\}$ be a dashed edge. Let $X_\alpha = D_p$ (or $D_p(\theta')$) and $X_\beta = I \times S_p$. Then $\phi_e^* \omega_{S^{n-1}}$ depends on only on the variable $x_{\sigma^{-1}(\alpha)} \in X_\alpha$ and on the first factor $r_{\sigma^{-1}(\beta)} \in I$ of $x_{\sigma^{-1}(\beta)} = (r_{\sigma^{-1}(\beta)}, \theta_{\sigma^{-1}(\beta)}) \in X_\beta$.*

**Proof** This follows from the way we choose the scaling of planetary orbits. □

**Definition 7.8** (graph-chord pairing) Let $C$ be a chord diagram on directed lines of order $k$. Let $\Gamma$ be a labeled BCR graph of order $k$. Then the pairing $\langle \Gamma, C \rangle$ is defined by counting as follows. First, we only count when

(I) $\#B(\Gamma) = 2k (= \#V(C))$.

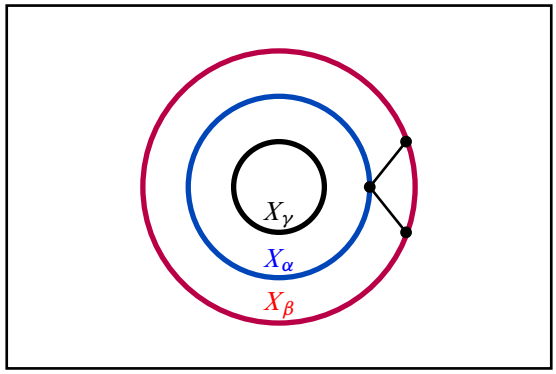


Figure 18: Outgoing edges.

Let $\#B(\Gamma) = \#V(C) = 2k$. We count permutations $\sigma : \#B(\Gamma) \to \#V(C)$ which satisfy (I) and all of the following:

(II) $\sigma$ induces the map $\bar{\sigma} : E(\Gamma) \to E(C)$.

(III) If two black vertices $v_1$ and $v_2$ are in the same solid component, $\sigma(v_1)$ and $\sigma(v_2)$ are on the same directed line.

(IV) If a vertex $w$ of $V(C)$ is not on the $x$-axis, $w$ has an ingoing solid edge: there exists a vertex $w'$ lower on the same directed line such that $\sigma^{-1}(w)$ and $\sigma^{-1}(w')$ are connected by some solid edge of $\Gamma$.

The sign of the counting is $+1$ if and only if the orientation of $\Gamma$ coincides with the induced orientation determined by the induced label from $\sigma$. (See Definition 7.9.)

**Definition 7.9** (induced label on BCR diagrams) Let $\sigma : B(\Gamma) \to V(C)$ satisfy conditions (I)–(IV) of Definition 7.8. Then $\sigma$ defines an induced label on the underlying graph $\overline{\Gamma}$ in a natural way: We order black vertices using $\sigma$ and the ordering of $V(C)$. (See Definition 6.4.) We orient solid edges so that the orientations are compatible with directed lines. We orient dashed edges so that the orientations are compatible with those of chords. We order edges as follows:

(1) Ingoing solid edge (if it exists) from the initial vertex of the $i^{\text{th}}$ chord ($i = 1, \dots, k$). There are $(g-1)$ solid edges ordered by this first step.

(2) The $\bar{\sigma}^{-1}(i)^{\text{th}}$ dashed edge and the ingoing solid edge from the target point of the $i^{\text{th}}$ chord ($i = 1, \dots, k$).

**Remark 7.10** We do not use the induced ordering of edges when $(n, j) = (\text{odd}, \text{odd})$.

**Theorem 7.11** (refer to [29, Lemma 4.12]) *Let $C$ be a chord diagram of order $k$ associated with a generalized ribbon cycle $\psi$. Assume $r(c)$ chords have the negative sign. Let $\Gamma$ be a BCR graph of order $k$. Then the value of the integral $I(\Gamma)$ on $\psi$ is equal to the pairing $(-1)^{r(c)}\langle \Gamma, C \rangle$.*

**Proof** By the localizing lemma, Lemma 7.2, the pairing lemma, Lemma 7.3, the same system lemma, Lemma 7.4, and the ingoing lemma, Lemma 7.6, respectively, the integral survives only on $C_\sigma$ for $\sigma$ which satisfies (I)–(IV) of Definition 7.8. By the decomposing lemma, Lemma 7.7, the integral on $C_\sigma$ can be written as

$$\pm(-1)^{r(c)}\left(\int_{\theta'_j\in S}\bigwedge_{j=1}^{g-1}\eta_{\tau(j)}\right)\left(\bigwedge_i\int_{x_{\sigma^{-1}(2i-1)}\in D_{p_i}}\int_{r_{\sigma^{-1}(2i)}\in I}\omega_{p_i}\int_{\theta_{\sigma^{-1}(2i)}\in S_{p_i}}\eta_{p_i}\right).$$

Here $\omega_{p_i}$ is the form associated with the dashed edge $\{x_{\sigma^{-1}(2i-1)}, x_{\sigma^{-1}(2i)}\}$. $\eta_{p_i}$ is the form associated with the solid edge that goes down from $x_{\sigma^{-1}(2i)}$. The form $\eta_{\tau(j)}$ is associated with the solid edge that goes down from $x_{\tau(j)}$. The sign at the head is $+$ if and only if the orientation of the configuration space $C_\sigma$ coincides with the orientation induced by the coordinate $(x_{\sigma^{-1}(1)}, x_{\sigma^{-1}(2)}, \dots, x_{\sigma^{-1}(2k)})$, and $\omega(\Gamma)$ is exactly $\bigwedge_{j=1}^{g-1}\eta_{\tau(j)}\wedge\bigwedge(\omega_{p_i}\eta_{p_i})$.

Recall that the image of the annulus $I\times S_{p_i}$ is perturbed to the direction $y_i\in S^{n-j-2}$. Then, in the part $\int_{x\in D}\int_{r\in I}\theta$, the linking number of $D$ and $\bigcup_{y_i\in S^{n-j-2}} I(y_i)$ is computed. Since this link is the Hopf link $S^{j-1}\cup\Sigma S^{n-j-2}\hookrightarrow\mathbb{R}^n$, the linking number is $+1$ or $-1$ depending on the sign of the chord. □

**Notation 7.12** Let $C=(\{t_i\}_{i=1,\dots,s},\{p_i\}_{i=1,\dots,k})$ be a chord diagram on directed lines. Let $G(C)$ be the set of BCR graphs (without a label) mapped on $C$ satisfying all the conditions of Definition 7.8.

**Lemma 7.13** *$G(C)$ consists of $\sum_{i=1}^{s}2^{t_i-1}$ graphs.*

**Proof** Since dashed edges must be mapped on chords, the remaining choices are solid edges. The top vertex $v$ on each directed line must be one of the ends of some solid component. The solid component first goes down from $v$ to $O$ through some of the vertices on the directed line. After reaching $O$, the solid component goes up though the remaining vertices. We can choose which of $(t_i-1)$ vertices between $v$ and $O$ the solid component passes when it goes down. □

## 7.2 The counting formula of configuration space integrals

**Theorem 7.14** (counting formula) *Let $H=\sum w(\Gamma_i)\Gamma_i$ be a graph cocycle that consists of $g$-loop graphs of order $k$. Let $C$ be a chord diagram on directed lines of order $k$, with $r(C)$ chords of negative sign. Let $\psi$ be a generalized ribbon cycle constructed from $C$. Then*

$$I(H)(\psi)=(-1)^{r(C)}\sum_{\overline{\Gamma}\in G(C)}w(\Gamma)\#\operatorname{Aut}(\overline{\Gamma})s(\Gamma,\overline{\Gamma}).$$

*Here $\Gamma$ is a labeled graph in $H$ such that the underlying graph of $\Gamma$ is $\overline{\Gamma}$. The sign $s(\Gamma,\overline{\Gamma})\in\{+1,-1\}$ is 1 if and only if the orientation of $\Gamma$ coincides with that of $\overline{\Gamma}$ with the induced label.*

**Proof** This follows from Theorem 7.11 and the symmetry lemma, Lemma 7.1. □

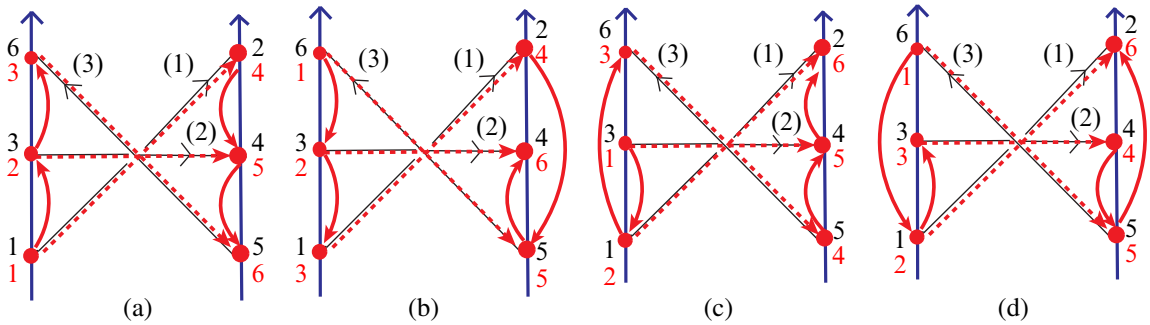


Figure 19: BCR graphs of $G(C_2)$.

**Example 7.15** For the chord diagram

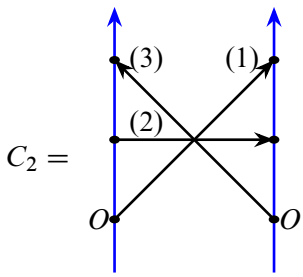


$G(C_2)$ consists of the four graphs drawn in red in Figure 19. The first BCR graph (a) is:

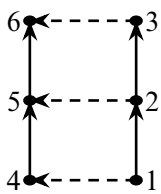

The other three graphs, (b), (c) and (d), are:

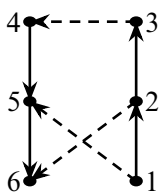

The induced label is written in black. The sign $s(\Gamma, \overline{\Gamma})$ is (a) $-1$, (b) $+1$, (c) $+1$ and (d) $-1$, respectively.

## 7.3 Cancellation of correction terms

Finally, we see lemmas for canceling the contribution of the collection term $\bar{c}(H)$.

**Lemma 7.16** [29, Lemma 4.13] *Let $\bar{\psi}: X \to \overline{\mathrm{Emb}}(\mathbb{R}^j, \mathbb{R}^n)$ be a generalized ribbon cycle of order $k$, and let $p_1, p_2, \ldots, p_k$ be its crossings. Then there exists a cycle $\bar{\psi}_0: X \to \overline{\mathrm{Emb}}(\mathbb{R}^j, \mathbb{R}^n)$ satisfying the following*:

- *$\bar{\psi}_0$ is obtained from $\bar{\psi}$ by resolving all crossings.*
- *The two differentials $D\bar{\psi}_0, D\bar{\psi}\colon [0,1]\times C_1(\mathbb{R}^j)\times X \to \mathrm{Inj}(\mathbb{R}^j,\mathbb{R}^n)$ are homotopic through an isotopy of $C_1(\mathbb{R}^j)$ that has a support in small neighborhoods of balls of crossings.*

**Lemma 7.17** *The cycle $\bar{\psi}_0$ satisfies the following.*

(1) $\bar{c}(H)(\bar{\psi}-\bar{\psi}_0)=0$.

(2) $I(H)(r_*\bar{\psi}_0)=0$, *where* $r\colon \overline{\mathrm{Emb}}(\mathbb{R}^j,\mathbb{R}^n)\to \mathrm{Emb}(\mathbb{R}^j,\mathbb{R}^n)$ *is the natural projection.*

(3) $\bar{\psi}_0$ *is a null-homotopic cycle.*

**Proof** For (1), recall that $\bar{c}(H)$ depends only on the differential

$$\overline{D}\colon [0,1]\times C_1(\mathbb{R}^j)\times \overline{\mathrm{Emb}}(\mathbb{R}^j,\mathbb{R}^n)\to \mathrm{Inj}(\mathbb{R}^j,\mathbb{R}^n),$$

and $\bar{c}(H)$ is defined as the fiber integral of the pullback of some closed form $\omega$ on $\mathrm{Inj}(\mathbb{R}^j,\mathbb{R}^n)$. By the second property of Lemma 7.16, the two compositions $D\bar{\psi}_0=\overline{D}\circ(\mathrm{id}_{[0,1]}\times \mathrm{id}_{C_1(\mathbb{R}^j)}\times\bar{\psi}_0)$ and $D\bar{\psi}=\overline{D}\circ(\mathrm{id}_{[0,1]}\times \mathrm{id}_{C_1(\mathbb{R}^j)}\times\bar{\psi})$ differ only in small neighborhoods of balls of crossings. Moreover, observe that neither $D\bar{\psi}_0$ nor $D\bar{\psi}$ depend on the parameter space $X$, in these small neighborhoods of balls. Hence by a dimensional reason, the integral vanishes on these neighborhoods. So we have (1). Parts (2) and (3) are due to the first property of Lemma 7.16. □

**Corollary 7.18** $$(r^*I(H)+\bar{c}(H))(\bar{\psi})=I(H)(\psi).$$

**Proof** By Lemma 7.17(1), (2) and (3), we have

$$\begin{aligned}(r^*I(H)+\bar{c}(H))(\bar{\psi}) &= (r^*I(H)+\bar{c}(H))(\bar{\psi}-\bar{\psi}_0) && \text{(by (3))}\\ &= (r^*I(H))(\bar{\psi}-\bar{\psi}_0) && \text{(by (1))}\\ &= I(H)(\psi) && \text{(by (2)).}\end{aligned}$$ □

**Remark 7.19** In particular, we have $\bar{c}(H)(\bar{\psi})=0$. We can show this directly without using $\bar{\psi}_0$, if we make the argument of the proof of (1) more precise: the parameter that runs on $S^{n-j-2}$ only affects a small neighborhood of the annulus of exactly one crossing; so if the cycle $\bar{\psi}$ has at least two crossings, the integral $\bar{c}(H)(\bar{\psi})$ vanishes by a dimensional reason.

## 8 Proof of the main result

Finally, we perform the pairing between the cocycle given in Section 4 and the cycle given in Section 6, and prove Theorem 3.1 and Corollary 3.4. The following completes the proof of Theorem 3.1.

**Theorem 8.1** $$\bar{z}_2^3(\bar{\psi})=1.$$

**Proof** By Corollary 7.18,

$$\bar{z}_2^3(\bar{\psi}) = I(H)(\psi).$$

Observe that the underlining graph of

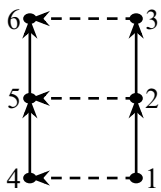


has 4 automorphisms, and the underlining graph of

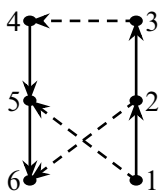


has 2 automorphisms. In the graph cocycle $H$,

$$w\left(\begin{array}{c}\text{6}\bullet\!\!-\!\!-\!\!-\!\!-\bullet\text{3}\\ \text{5}\bullet\!\!-\!\!-\!\!-\!\!-\bullet\text{2}\\ \text{4}\bullet\!\!-\!\!-\!\!-\!\!-\bullet\text{1}\end{array}\right) = -\frac{1}{4} \qquad \text{and} \qquad w\left(\begin{array}{c}\text{4}\bullet\!\!-\!\!-\!\!-\!\!-\bullet\text{3}\\ \text{5}\bullet\!\!-\!\!-\!\!-\!\!-\bullet\text{2}\\ \text{6}\bullet\!\!-\!\!-\!\!-\!\!-\bullet\text{1}\end{array}\right) = -1.$$

Hence by the counting formula, Theorem 7.14, and Example 7.15,

$$I(H)(\psi) = -\sum_{\overline{\Gamma}\in G(C_2)} w(\Gamma)\#\operatorname{Aut}(\overline{\Gamma})s(\Gamma,\overline{\Gamma}) = -\left(-\tfrac{1}{4}\times 4\times(-1)+(-1)\times 2\times(+1+1-1)\right) = 1. \quad \square$$

**Remark 8.2** We can give a simpler proof of Theorem 8.1 using graph homology [29]. We give a sketch of the proof here. Let $\mathcal{A}(k,g)$ be the graph homology generated by $g$-loop BCR graphs of order $k$. Let $\overline{w}\colon \mathcal{A}(k,g)\to\mathbb{R}$ be a weight system on it. Then

$$H = \sum_{\substack{\overline{\Gamma}\\ k(\overline{\Gamma})=k, g(\overline{\Gamma})=g}} \frac{\overline{w}(\Gamma)}{\#\operatorname{Aut}(\overline{\Gamma})}\Gamma$$

is a graph cocycle. Set

$$w(\Gamma) = \frac{\overline{w}(\Gamma)}{\#\operatorname{Aut}(\overline{\Gamma})}.$$

Then the counting formula, Theorem 7.14, says

$$I(H)(\psi) = (-1)^{r(C)} \sum_{\overline{\Gamma}\in G(C)} \overline{w}(\Gamma)s(\Gamma,\overline{\Gamma}).$$

Consider the weight system $\overline{w}\colon \mathcal{A}(3,2) \to \mathbb{R}$ such that

$\overline{w}\Big($ 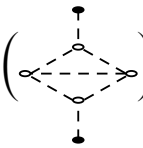 $\Big) = \pm 1.$

Observe that the linear combination of four graphs $\sum_{\overline{\Gamma}\in G(C_2)} s(\Gamma,\overline{\Gamma})\Gamma$ gives the same class as the hairy graph

$\pm$ 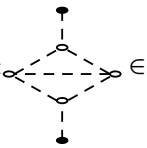 $\in \mathcal{A}(3,2).$

(To see this, use STU relations.) Then we have

$$I(H)(\psi) = (-1)^{r(C_2)}\overline{w}\Big(\sum_{\overline{\Gamma}\in G(C_2)} s(\Gamma,\overline{\Gamma})\Gamma\Big) = \pm\overline{w}\Big($$ 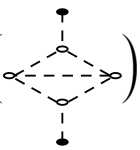 $$\Big) \neq 0.$$

Finally, we prove Corollary 3.4, the case $n-j-2=0$. Let

$$\bar{\psi}(0,0,0)\colon S^{j-1} \to \overline{\mathrm{Emb}}(\mathbb{R}^j,\mathbb{R}^{j+2})$$

be the $(0,0,0)\in S^0\times S^0\times S^0$ component of $\bar{\psi}$, that is, the component where no crossing is resolved. By Proposition 6.10, $\bar{\psi}(0,0,0)$ is in the unknot component (the path component of the trivial path of the trivial immersion).

**Corollary 8.3** *When $n-j=2$, $\bar{\psi}$ and $\bar{\psi}(0,0,0)$ give the same homology class. Hence, when $j$ is odd, $\bar{\psi}$ gives an nontrivial element of*

$$\pi_*(\overline{\mathrm{Emb}}(\mathbb{R}^j,\mathbb{R}^{j+2})_\iota)\otimes\mathbb{Q}.$$

**Proof** Since $S_0=\{x_3=0,x_3=2\}$, we write

$$\bar{\psi} = \sum_{\epsilon_i\in\{0,2\}} \bar{\psi}(\varepsilon_1,\varepsilon_2,\varepsilon_3).$$

Observe that if one of $\varepsilon_i$ is 2, $\bar{\psi}(\varepsilon_1,\varepsilon_2,\varepsilon_3)$ is a degenerate cycle. □

## References


[1] **V I Arnold**, *The cohomology ring of the colored braid group*, Mat. Zametki 5 (1969) 227–231 MR Zbl In Russian; translated in Math. Notes 5 (1969) 138–140

[2] **G Arone**, **V Turchin**, *On the rational homology of high-dimensional analogues of spaces of long knots*, Geom. Topol. 18 (2014) 1261–1322 MR Zbl

[3] **G Arone**, **V Turchin**, *Graph-complexes computing the rational homotopy of high dimensional analogues of spaces of long knots*, Ann. Inst. Fourier (Grenoble) 65 (2015) 1–62 MR Zbl

[4] **S Axelrod**, **I M Singer**, *Chern–Simons perturbation theory, II*, J. Differential Geom. 39 (1994) 173–213 MR Zbl

[5] **D Bar-Natan**, *On the Vassiliev knot invariants*, Topology 34 (1995) 423–472 MR Zbl

[6] **R Bott**, *Configuration spaces and imbedding invariants*, Turkish J. Math. 20 (1996) 1–17 MR Zbl

[7] **R Bott**, **C Taubes**, *On the self-linking of knots*, J. Math. Phys. 35 (1994) 5247–5287 MR Zbl

[8] **R Budney**, *A family of embedding spaces*, from "Groups, homotopy and configuration spaces", Geom. Topol. Monogr. 13, Geom. Topol. Publ., Coventry (2008) 41–83 MR Zbl

[9] **R Budney**, **D Gabai**, *Knotted 3-balls in $S^4$*, preprint (2019) arXiv 1912.09029

[10] **A S Cattaneo**, **P Cotta-Ramusino**, **R Longoni**, *Configuration spaces and Vassiliev classes in any dimension*, Algebr. Geom. Topol. 2 (2002) 949–1000 MR Zbl

[11] **A S Cattaneo**, **C A Rossi**, *Wilson surfaces and higher dimensional knot invariants*, Comm. Math. Phys. 256 (2005) 513–537 MR Zbl

[12] **J Conant**, **J Costello**, **V Turchin**, **P Weed**, *Two-loop part of the rational homotopy of spaces of long embeddings*, J. Knot Theory Ramifications 23 (2014) art. id. 1450018 MR Zbl

[13] **B Fresse**, **V Turchin**, **T Willwacher**, *The rational homotopy of mapping spaces of $E_n$ operads*, preprint (2017) arXiv 1703.06123

[14] **T G Goodwillie**, **J R Klein**, **M S Weiss**, *Spaces of smooth embeddings, disjunction and surgery*, from "Surveys on surgery theory, II", Ann. of Math. Stud. 149, Princeton Univ. Press (2001) 221–284 MR Zbl

[15] **T G Goodwillie**, **M Weiss**, *Embeddings from the point of view of immersion theory, II*, Geom. Topol. 3 (1999) 103–118 MR Zbl

[16] **K Habiro**, **T Kanenobu**, **A Shima**, *Finite type invariants of ribbon 2-knots*, from "Low-dimensional topology", Contemp. Math. 233, Amer. Math. Soc., Providence, RI (1999) 187–196 MR Zbl

[17] **K Habiro**, **A Shima**, *Finite type invariants of ribbon 2-knots, II*, Topology Appl. 111 (2001) 265–287 MR Zbl

[18] **M Kontsevich**, *Feynman diagrams and low-dimensional topology*, from "First European Congress of Mathematics, II", Progr. Math. 120, Birkhäuser, Basel (1994) 97–121 MR Zbl

[19] **G Kuperberg**, **D P Thurston**, *Perturbative 3-manifold invariants by cut-and-paste topology*, preprint (1999) arXiv math/9912167

[20] **C Lescop**, *On the Kontsevich–Kuperberg–Thurston construction of a configuration-space invariant for rational homology 3-spheres*, preprint (2004) arXiv math/0411088

[21] **C Lescop**, *Invariants of links and 3-manifolds from graph configurations*, preprint (2020) arXiv 2001.09929

[22] **D Leturcq**, *Generalized Bott–Cattaneo–Rossi invariants of high-dimensional long knots*, J. Math. Soc. Japan 73 (2021) 815–860 MR Zbl

[23] **R Longoni**, *Nontrivial classes in $H^*(\mathrm{Imb}(S^1, \mathbb{R}^n))$ from nontrivalent graph cocycles*, Int. J. Geom. Methods Mod. Phys. 1 (2004) 639–650 MR Zbl

[24] **M Mimura**, **H Toda**, *Topology of Lie groups: I, II*, Transl. Math. Monogr. 91, Amer. Math. Soc., Providence, RI (1991) MR Zbl

[25] **K E Pelatt**, **D P Sinha**, *A geometric homology representative in the space of knots*, from "Manifolds and $K$–theory", Contemp. Math. 682, Amer. Math. Soc., Providence, RI (2017) 167–188 MR Zbl

[26] **K Sakai**, *Nontrivalent graph cocycle and cohomology of the long knot space*, Algebr. Geom. Topol. 8 (2008) 1499–1522 MR Zbl

[27] **K Sakai**, *Configuration space integrals for embedding spaces and the Haefliger invariant*, J. Knot Theory Ramifications 19 (2010) 1597–1644 MR Zbl

[28] **K Sakai**, *An integral expression of the first nontrivial one-cocycle of the space of long knots in* $\mathbb{R}^3$, Pacific J. Math. 250 (2011) 407–419 MR Zbl

[29] **K Sakai**, **T Watanabe**, *1-loop graphs and configuration space integral for embedding spaces*, Math. Proc. Cambridge Philos. Soc. 152 (2012) 497–533 MR Zbl

[30] **D P Sinha**, *Manifold-theoretic compactifications of configuration spaces*, Selecta Math. 10 (2004) 391–428 MR Zbl

[31] **D P Sinha**, *The (non-equivariant) homology of the little disks operad*, from "OPERADS 2009", Sémin. Congr. 26, Soc. Math. France, Paris (2013) 253–279 MR Zbl

[32] **T Watanabe**, *Configuration space integral for long n-knots and the Alexander polynomial*, Algebr. Geom. Topol. 7 (2007) 47–92 MR Zbl

[33] **T Watanabe**, *On Kontsevich's characteristic classes for higher dimensional sphere bundles, I: The simplest class*, Math. Z. 262 (2009) 683–712 MR Zbl

[34] **T Watanabe**, *On Kontsevich's characteristic classes for higher-dimensional sphere bundles, II: Higher classes*, J. Topol. 2 (2009) 624–660 MR Zbl

[35] **T Watanabe**, *Higher order generalization of Fukaya's Morse homotopy invariant of 3-manifolds, I: Invariants of homology 3-spheres*, Asian J. Math. 22 (2018) 111–180 MR Zbl

[36] **T Watanabe**, *Some exotic nontrivial elements of the rational homotopy groups of* $\mathrm{Diff}(S^4)$, preprint (2018) arXiv 1812.02448

[37] **T Watanabe**, *Theta-graph and diffeomorphisms of some 4-manifolds*, preprint (2020) arXiv 2005.09545

[38] **M Weiss**, *Embeddings from the point of view of immersion theory, I*, Geom. Topol. 3 (1999) 67–101 MR Zbl

[39] **E Witten**, *Quantum field theory and the Jones polynomial*, Comm. Math. Phys. 121 (1989) 351–399 MR Zbl

*Graduate School of Mathematical Sciences, The University of Tokyo*
*Tokyo, Japan*

yoshioka@ms.u-tokyo.ac.jp

Received: 28 February 2023 Revised: 10 May 2024

# ALGEBRAIC & GEOMETRIC TOPOLOGY

msp.org/agt



## EDITORS

PRINCIPAL ACADEMIC EDITORS

John Etnyre
etnyre@math.gatech.edu
Georgia Institute of Technology

Kathryn Hess
kathryn.hess@epfl.ch
École Polytechnique Fédérale de Lausanne

BOARD OF EDITORS

| | | | |
|---|---|---|---|
| Julie Bergner | University of Virginia<br>jeb2md@eservices.virginia.edu | Thomas Koberda | University of Virginia<br>thomas.koberda@virginia.edu |
| Steven Boyer | Université du Québec à Montréal<br>cohf@math.rochester.edu | Markus Land | LMU München<br>markus.land@math.lmu.de |
| Tara E Brendle | University of Glasgow<br>tara.brendle@glasgow.ac.uk | Christine Lescop | Université Joseph Fourier<br>lescop@ujf-grenoble.fr |
| Indira Chatterji | CNRS & Univ. Côte d'Azur (Nice)<br>indira.chatterji@math.cnrs.fr | Norihiko Minami | Yamato University<br>minami.norihiko@yamato-u.ac.jp |
| Octav Cornea | Université' de Montreal<br>cornea@dms.umontreal.ca | Andrés Navas | Universidad de Santiago de Chile<br>andres.navas@usach.cl |
| Alexander Dranishnikov | University of Florida<br>dranish@math.ufl.edu | Robert Oliver | Université Paris 13<br>bobol@math.univ-paris13.fr |
| Tobias Ekholm | Uppsala University, Sweden<br>tobias.ekholm@math.uu.se | Jessica S Purcell | Monash University<br>jessica.purcell@monash.edu |
| Mario Eudave-Muñoz | Univ. Nacional Autónoma de México<br>mario@matem.unam.mx | Birgit Richter | Universität Hamburg<br>birgit.richter@uni-hamburg.de |
| David Futer | Temple University<br>dfuter@temple.edu | Jérôme Scherer | École Polytech. Féd. de Lausanne<br>jerome.scherer@epfl.ch |
| John Greenlees | University of Warwick<br>john.greenlees@warwick.ac.uk | Vesna Stojanoska | Univ. of Illinois at Urbana-Champaign<br>vesna@illinois.edu |
| Matthew Hedden | Michigan State University<br>mhedden@math.msu.edu | Zoltán Szabó | Princeton University<br>szabo@math.princeton.edu |
| Kristen Hendricks | Rutgers University<br>kristen.hendricks@rutgers.edu | Maggy Tomova | University of Iowa<br>maggy-tomova@uiowa.edu |
| Hans-Werner Henn | Université Louis Pasteur<br>henn@math.u-strasbg.fr | Daniel T Wise | McGill University, Canada<br>daniel.wise@mcgill.ca |
| Daniel Isaksen | Wayne State University<br>isaksen@math.wayne.edu | Lior Yanovski | Hebrew University of Jerusalem<br>lior.yanovski@gmail.com |



See inside back cover or msp.org/agt for submission instructions.

The subscription price for 2025 is US $760/year for the electronic version, and $1110/year (+$75, if shipping outside the US) for print and electronic. Subscriptions, requests for back issues and changes of subscriber address should be sent to MSP. Algebraic & Geometric Topology is indexed by Mathematical Reviews, Zentralblatt MATH, Current Mathematical Publications and the Science Citation Index.

Algebraic & Geometric Topology (ISSN 1472-2747 printed, 1472-2739 electronic) is published 9 times per year and continuously online, by Mathematical Sciences Publishers, c/o Department of Mathematics, University of California, 798 Evans Hall #3840, Berkeley, CA 94720-3840. Periodical rate postage paid at Oakland, CA 94615-9651, and additional mailing offices. POSTMASTER: send address changes to Mathematical Sciences Publishers, c/o Department of Mathematics, University of California, 798 Evans Hall #3840, Berkeley, CA 94720-3840.

AGT peer review and production are managed by EditFlow® from MSP.

PUBLISHED BY

mathematical sciences publishers

nonprofit scientific publishing

https://msp.org/



© 2025 Mathematical Sciences Publishers

ALGEBRAIC & GEOMETRIC TOPOLOGY

Volume 25 Issue 6 (pages 3145–3787) 2025

Holomorphic polygons and the bordered Heegaard Floer homology of link complements 3145

THOMAS HOCKENHULL

Exact Lagrangian tori in symplectic Milnor fibers constructed with fillings 3225

ORSOLA CAPOVILLA-SEARLE

A note on embeddings of 3-manifolds in symplectic 4-manifolds 3251

ANUBHAV MUKHERJEE

A note on knot Floer homology of satellite knots with (1, 1)-patterns 3271

WEIZHE SHEN

A $K$-theory spectrum for cobordism cut and paste groups 3287

RENEE S HOEKZEMA, CARMEN ROVI and JULIA SEMIKINA

The Curtis–Wellington spectral sequence through cohomology 3315

DANA HUNTER

The slices of quaternionic Eilenberg–Mac Lane spectra 3341

BERTRAND J GUILLOU and CARISSA SLONE

Cocycles of the space of long embeddings and BCR graphs with more than one loop 3385

LEO YOSHIOKA

Asymptotic cones of snowflake groups and the strong shortcut property 3429

CHRISTOPHER H CASHEN, NIMA HODA and DANIEL J WOODHOUSE

Whitney tower concordance and knots in homology spheres 3503

CHRISTOPHER W DAVIS

The asymptotic behaviors of the colored Jones polynomials of the figure-eight knot, and an affine representation 3523

HITOSHI MURAKAMI

The Goldman bracket characterizes homeomorphisms between noncompact surfaces 3585

SUMANTA DAS, SIDDHARTHA GADGIL and AJAY KUMAR NAIR

A geometric computation of cohomotopy groups in codegree one 3603

MICHAEL JUNG and THOMAS O ROT

Calabi–Yau structure on the Chekanov–Eliashberg algebra of a Legendrian sphere 3627

NOÉMIE LEGOUT

On the resolution of kinks of curves on punctured surfaces 3679

CHRISTOF GEISS and DANIEL LABARDINI-FRAGOSO

Weinstein presentations for high-dimensional antisurgery 3707

IPSITA DATTA, OLEG LAZAREV, CHINDU MOHANAKUMAR and ANGELA WU

Singular Legendrian unknot links and relative Ginzburg algebras 3737

JOHAN ASPLUND

An RBG construction of integral surgery homeomorphisms 3755

QIANHE QIN

Powell's conjecture on the Goeritz group of $S^3$ is stably true 3775

MARTIN SCHARLEMANN